

TESTING OF THE INTER-TURN INSULATION OF HIGH VOLTAGE INDUCTION
MOTOR COILS

Michael John Hopkins

A Dissertation Submitted to the Faculty of Engineering
University of the Witwatersrand, Johannesburg
for the Degree of Master of Science

Johannesburg 1976

ABSTRACT

It is recognised that a need exists for a reliable set of tests of induction motor coil inter-turn insulation, due to the dangers presented to such insulation by fast rising surges. The occurrence and form of such surges are discussed. The behaviour of surges on coils is analysed both in theory and in practice to derive the maximum stress likely to be imposed on a coil by a fast rising surge. Based on this a criterion is proposed for inter-turn tests.

Two tests which do not require the coil to be cut, are proposed. The first consists of discharging a charged capacitor through the coil and allowing a damped oscillation to occur which effectively stresses the inter-turn insulation. The second test consists of inducing a high frequency voltage wave into the coil using an electronic oscillator. Refinements are proposed for both tests to allow for a production test programme as well as to permit an unambiguous detection of breakdown between turns. A number of test circuits are proved in practice. Tests are derived to assess the validity and safety of the capacitor discharge test. A number of materials and samples are tested to assess their behaviour in the proposed inter-turn tests. The results of such tests are compared with those obtained with the standard impulse test. The breakdown process between the turns of a coil is examined and analysed to reveal a weakness in induction motor coils which can lead to a reduced resistance to inter-turn breakdown.

I, Michael John Hopkins do state that this dissertation
is my own unaided work and has not been presented in whole
or in part for any other degree or at any other university.

M. J. Hopkins

ACKNOWLEDGEMENT

The author wishes to thank GEC Machines (Pty) Ltd. and Marthinusen Ltd. for assistance and materials supplied.

<u>CONTENTS</u>	PAGE
1 INTRODUCTION	1
2 AN ANALYSIS OF IMPULSES LIKELY TO STRESS THE INTER-TURN INSULATION OF MOTORS	3
3 THEORETICAL BEHAVIOUR OF SURGES ON MOTOR COILS ..	6
4 TRANSIENT MEASUREMENTS ON COILS USING LOW VOLTAGE SURGES	17
4.1 Model Coils - Results	19
4.2 Commercially Produced Motor Coils	26
5 THE CAPACITIVE DISCHARGE TEST	32
5.1 Introduction	32
5.2 A Practical Capacitive Discharge Test ..	38
5.3 Detection of Breakdown in the Capacitive Discharge Test	47
5.4 An Improved Test Suitable for Factory Use ..	55
5.5 Statistical Tests on the Capacitor Discharge Method.. .. .	58
5.6 Various Effects Observed Concerning the Capacitive Discharge Test	65
5.6.1 The Discharge between Turns	65
5.6.2 Noise on the Discharge Waveform ..	68
6 RADIO FREQUENCY COIL TESTING	70
7 PRACTICAL BREAKDOWN TESTS PERFORMED ON A NUMBER OF INSULATING MATERIALS	81
7.1 Introduction	81
7.2 Tests on Real Coil Samples	81
7.3 Tests using Sheet Samples of Insulating Materials	86
7.4 Analysis of the Test Results	90
7.4.1 Impulse Tests	90
7.4.2 Radio Frequency Tests	96

					PAGE	
8	CONCLUSION	98
	APPENDIX A	101
	APPENDIX B	104
	APPENDIX C	106
	APPENDIX D	109
	APPENDIX E	111
	REFERENCES	129

1 INTRODUCTION

Insulation breakdown is the most feared failure occurring in large high voltage induction motors. Damage to the ground insulation is often extensive, and it is the breakdown of this insulation which is most often cited as the initial cause of the damage. In some cases, however, it is suspected that the initial failure occurs between turns; heat generation at this point weakens the ground insulation which fails catastrophically destroying all evidence of the initial failure. [1]

It has been noticed by local manufacturers and repairers that the incidence of insulation failure is much higher during summer. [2] As the South African industrial areas are subjected to a large amount of lightning during this season it is likely that lightning surges are the root cause of this trouble, by the above process. Lightning surges can travel into the windings, which because of their distributed parameters, behave in a similar fashion to a transmission line. The steep surge front is imposed across a coil (or even a few turns) causing a high transient stress of the insulation between turns. If this insulation has only been designed to withstand the normal working potential between turns of at the most a few hundred volts, or if the coil is faulty, then inter-turn failure is likely.

To ensure a reliable motor all manufacturers test the insulation during and after manufacture. This is usually only done for strength of ground insulation, as testing of interturn insulation is difficult, especially before the coils have been installed in the stator.

At present the usual method of impulse testing interturn insulation of motor coils is to cut a coil yielding a number of parallel conductors which are then impulsed using the normal type of impulse generator. Such a test is specified by both The Rand Water Board and ESCOM. (ESCOM spec. DCS 1551) The major defect of this test is that it destroys the coil, whether sound or unsound. Considering the high cost of manufacturing such coils, most firms are loath to use it. It is suitable for locating

design defects, or for locating systematic defects in batches of coils. As it cannot be applied to every coil it cannot locate the isolated coil with a latent defect. Furthermore, it is a tedious test requiring a skilled operator. The process of cutting the coil may also damage the insulation, making the test invalid.

A test is therefore required which is non-destructive to all but unsound coils. It should be both safe and easy to apply, and be suited to routine testing.

The prime limiting factor in inter-turn testing is the very low impedance of motor coils. At normal frequencies very high currents would be required to produce a suitable potential drop across the coil. The normal type of impulse generator is unsuitable due to its relatively high internal impedance. To increase the impedance of a coil, high frequencies are necessary. This can be done in two ways.

The first consists of discharging a high voltage capacitor into the inductance of the coil. The resulting LC combination executes damped oscillations which stress the coil insulation.

The second method uses an electronic valve circuit to generate high voltage radio frequency oscillations which are induced into the coil to stress the insulation.

There are decided advantages and disadvantages to both methods and an analysis of this is attempted. It is also proposed to analyse the nature of impulses encountered in practice as well as impulse behaviour on coils in an attempt to set a criterion for such tests and their ability to ensure a motor resistant to natural impulses.

2 AN ANALYSIS OF IMPULSES LIKELY TO STRESS THE INTER-TURN INSULATION OF MOTORS

Impulses travelling on transmission systems can be caused by a number of events [3]. These are basically either switching surges, or lightning induced impulses. The classic type of switching surges found on transmission lines are usually too slow to cause trouble [4,5]. However, vacuum quenched circuit breakers are being used increasingly for motor switching and can cause extremely fast transients to occur at the motor terminals due primarily to re-ignition phenomena [6,7]. Lightning surges can have very steep fronts and it is worthwhile considering studies undertaken on lightning in an effort to estimate the type of surge likely to cause distress to a motor's inter-turn insulation.

The shape of impulses used to test transformers have been specified by various bodies [8,9,10]. The rise times of such waves have been fixed by a semi-empirical process of considering the types of wave likely to be encountered in practice and deciding which is most dangerous to a transformer [11]. The waves chosen have rise times of the order of 1 microsec, which are representative of those likely to stress the transformer due to the nature of typical transformer insulations. Most transformers use liquid insulating mediums. These have long formative time lags for high voltage breakdown, of the order of 1 microsec. [12,13]. Thus a faster rise time would tend to stress the oil less and the value of rise time chosen will stress the inter-turn insulation of an oil-filled transformer maximally. Transformers tested on these assumptions have performed well in service.

Solid insulating materials have much shorter breakdown formative time lags, typically 10 to 100 nanoseconds [1]. They are, therefore, more sensitive to fast transients than liquid based insulations with slower formative time lags. When considering the type of wave likely to damage a motor, one is forced to give consideration to much faster fronted waves than one would normally consider with liquid-filled

transformers.

Lightning surges on transmission systems have been studied extensively [3,4,15,16,17,18,19,20] using various systems and techniques. The standard method is to use a cathode ray oscilloscope to monitor the potential across a divider chain connected to a transmission line. Times to crest vary from 0.1 to 40 microseconds, with most rise times in the region of 1 to 5 microseconds, supporting the choice of rise times used for transformer testing. Crest values were up to 6 times the working voltage of the line [3]. On modern systems this would be limited by arrester sparkover values, summarised in Appendix A. They are approximately three times the working voltage for a 1.2×50 microsec wave, but may be much higher for faster rise times as is indicated in the Appendix. It appears from the test waves considered in these specifications that a rise time of 0.1 microsec is not unlikely in practice, although this may be rather severe considering that there is no certainty that very fast waves go up to full arrester sparkover.

Work has also been done on estimating the maximum rate of rise of surges, using a magnetic link to measure the maximum charging current into a capacitor connected to the line [3]. Whilst no indication of wave shape is given, it may be assumed that a sizable proportion of the wave front has this slope. The following results were obtained for a number of lightning surges:

Line volts KV	Maximum of wave front K ¹ usec		
	maximum	average	minimum
132	N10	220	-
33	240	100	49
12	2N2	65	25

Of particular interest is the 12 KV line, similar to local 11 KV lines. For such lines values of up to 280 KV/microsecond could be considered.

Also to be noted are the specifications for arrester sparkover voltages on wave fronts (Appendix A). A 12 KV

arrester used normally on an 11 KV system has a sparkover at 50 KV when a wave rising at 100 KV/microsec is used. A wave of this rate of rise would appear to be not unknown in practice if it is specified for arrester tests.

In considering inter turn insulation it is the high rate of rise which does damage. This can be of the order of 100 to 300 KV/microsec for an 11 KV system. A useful value to adopt is thus 20 KV/microsec per KV of rating. The maximum value of the crest is unimportant for arrester-protected systems, but may be taken as a maximum of five times the supply rating.

In defence of such a rapid rate of rise it is interesting to study work done on currents in direct strokes [17,18,19, 20]. Current rates of rise can easily be of the order of 40 KA/microsec and these currents acting through the surge impedance of a line, or the footing impedance of a tower give rates of voltage rise which are extremely rapid. Also a study on 110 V systems [16] indicated rise times of as fast as 0.05 microsec with crests of up to 2 KV.

Vacuum circuit breakers, because of their advantages of compactness and reliability, have become popular for motor switching. They do have the disadvantage of tending to generate fast transients. These transients may be caused by pre-strike [6] or restrike [7] phenomena. The transients are commonly of the order of 1 microsecond risetime, but may have rise times as fast as 0.3 microseconds. The harmful effects of these transients may be avoided by careful design of the control gear or the use of filters. A study of re-strikes [7] has indicated rates of change of up to 5 KV per microsecond per KV of supply potential.

In conclusion it may be noted that no allowance has been made for chopped waves, which can have extremely high rates of change. Chopped waves are usually the result of poor arrester usage, being caused by flashover at an unprotected point. It is also worth noting that transformers are able to pass the high frequency components of surges due to the capacitive coupling of the winding. Thus transformers would appear to be not very effective in protecting motors from fast impulses [21].

3 THEORETICAL BEHAVIOUR OF SURGES ON MOTOR COILS

The ability of motor coils to withstand fast fronted surges requires not only a determination of the type of impulses likely to cause trouble, but also the behaviour of these impulses on entering a given motor coil. Mathematical analysis has been attempted in references [3,22,23,24,25,26,27,28,29,30], the first three being the most useful.

Qualitatively it is known that coils behave in a similar manner to transmission lines. This is due to the distributed nature of their parameters. Surges are able to travel in the coil and are transmitted through it, usually being extensively modified in the process. The differences between a coil and a transmission line lie basically in the coupling due to mutual inductance and capacitance in the coil. Any wave passing through is degraded, the higher frequency components of the wave front being particularly attenuated. The wave front tends to flatten out and thus only the first sections of a coil are fully stressed between turns.

The coil also presents a surge impedance which can be measured. This is frequency dependent, making an accurate determination difficult. This surge impedance, Z_c , can cause trouble if supplied from a line of impedance Z_1 . The terminal voltage then tends to change under surge conditions to

$$U = 2U \frac{Z_c}{Z_1 + Z_c}$$

where U is the crest value of a surge on the line. Thus an increase in surge potential can occur and flashover may occur near the machine terminals. If the end of the winding is not grounded or terminated then flashover may also occur here due to reflection of surges travelling through the windings.

The simplest approach to surge analysis is that of concentrating only on the first few turns of the coil and assuming that the surge does not materially change on passing through them. It is assumed to have a constant slope and

velocity. If this slope is M volts/sec then the voltage across the first turn is

$$\begin{aligned} V_{01} &= M T \\ &= M \frac{L_t}{v} \quad \text{volts} \dots\dots (1) \end{aligned}$$

where T is the transit time for a turn and L_t the length of each turn of the coil.

The surge velocity can be estimated to be that of a transmission line in the same medium as the coil. i.e.

$$v = \frac{C}{\sqrt{\epsilon_r}} \quad \text{metres/sec} \dots\dots (2)$$

where C is the velocity of the light and ϵ_r is the relative permittivity (dielectric constant) of the winding insulation. For a popular modern material such as epoxy resin and mica (or glass) the value of ϵ_r is 6, giving a velocity of

$$\begin{aligned} v &= \frac{3 \times 10^8}{6} \\ &= 1.2 \times 10^8 \quad \text{metres/sec} \end{aligned}$$

For example take an 11 KV coil with $L_t = 2$ metres and using a wave of slope $20 \times 11 = 220$ KV/microsec, to give the voltage across the first turn as

$$\begin{aligned} V_{01} &= 220 \times 10^6 \frac{2}{1.2 \times 10^8} \\ &= 3.6 \quad \text{KV/turn} \end{aligned}$$

and $T = 17$ nanoseconds

When one considers that the normal working stress is perhaps 100 V then the impulsive strain on this insulation can be appreciated.

This approach ignores the coupling between coil elements. Taking just the capacitive coupling gives the following model. This model is suitable only for the very high frequency components of the surge, i.e. the front of the very steep surge.

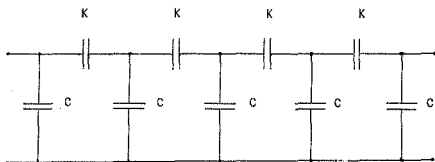


Figure 3.1 Capacitive model

K is capacity between turns
 C is capacity of turn to ground

This is the same as a string of n insulators and if the number of elements is high then the potential of any element, say m , is

$$V_m = U \frac{\text{Sinh } (n-m) q}{\text{Sinh } nq} \dots\dots\dots (3)$$

where $q = \sqrt{\frac{C}{K}}$, the transfer function.
 (See Appendix B)

For the first turn the potential is

$$V_1 = U \frac{\text{Sinh } (n-1) q}{\text{Sinh } nq} \dots\dots\dots (4)$$

and the potential across the first turn is

$$V_{01} = U \left(1 - \frac{\text{Sinh } (n-1) q}{\text{Sinh } nq} \right) \dots\dots (5)$$

If $(n-1) q$ is larger than 3 then

$$\text{Sinh } (n-1) q \approx \frac{e^{(n-1)q}}{2} \dots\dots\dots (6)$$

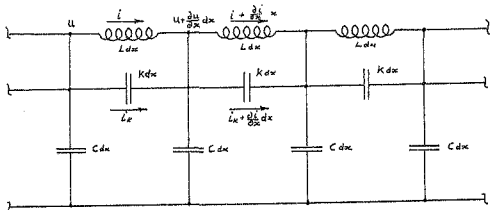
and

$$i_{k1} = U(1 - e^{-g}) \quad \dots \quad (7)$$

If g is small, a first order approximation results

$$i_{k1} = Ug \quad \dots \quad (8)$$

A more precise analysis of surge behavior is that due to Wagner [22]. He used a ladder network as in figure 3.2, taking into account all parameters except the mutual inductance between turns.



L = Inductance/unit length

C = Ground capacity/unit length

K = Turn capacity/unit length

Figure 3.2 Wagner's model

For an element of the coil winding the following relationships hold:

$$\partial(i + i_k) = -C \frac{\partial u}{\partial t} \quad \dots \quad (9)$$

$$i_k = -K \frac{\partial^2 u}{\partial x \partial t} \quad \dots \quad (10)$$

$$\frac{\partial u}{\partial x} = -L \frac{\partial i}{\partial t} \quad \dots \quad (11)$$

where u and i are respective voltages and currents

Eliminating the current terms

$$\frac{\partial^2 u}{\partial x^2} - LC \frac{\partial^2 u}{\partial t^2} + LK \frac{\partial^4 u}{\partial x^2 \partial t^2} = 0 \dots\dots (12)$$

Assuming a solution of the form

$$u = v e^{j\omega t} e^{j\alpha x} \dots\dots (13)$$

and substituting into (12) gives

$$\alpha^2 - LC\omega^2 - LK\alpha^2\omega^2 = 0 \dots\dots (14)$$

Solving for ω

$$\omega = \frac{\alpha}{\sqrt{LC(1 + \frac{K}{C}\alpha^2)}} \dots\dots (15)$$

and

$$= \frac{+}{-} \omega \sqrt{\left(\frac{LC}{1 - \omega^2 LK}\right)} \dots\dots (16)$$

Where α tends to infinity,

$$\omega = \frac{1}{\sqrt{LK}} \dots\dots (17)$$

= ω_{cr} , the critical frequency of the coil.

This is the highest frequency in the coil may freely oscillate. It is the natural frequency of an inductance L and a capacitance C. If a travelling wave solution is sought then such a wave will have a velocity,

$$v = \frac{\omega K}{\alpha^2} = \frac{+}{-} \frac{1}{\sqrt{LC(1 + \frac{K}{C}\alpha^2)}} \dots\dots (18)$$

i.e. if α tends to infinity then v tends to zero.

Above the critical frequency the velocity term is imaginary and thus the coil will pass only components below the critical frequency. In other words the coil acts as a low pass filter, tending to pass only frequencies below a certain value, the critical frequency. Like all filters this effect is not abrupt and higher frequencies tend to penetrate the coil to a certain extent.

A simpler approach may be found by considering one element of the coil shown in figure 3.2. If the inductive and inter-turn capacities are lumped the impedance to a wave of frequency ω is that of the two elements in parallel

$$\begin{aligned} \text{i.e. } Z &= \frac{X_L X_C}{X_L + X_C} \\ &= \frac{j\omega L}{1 - \omega^2 LK} \quad \dots\dots\dots (19) \end{aligned}$$

At a frequency

$$\omega = \frac{1}{\sqrt{LK}} \quad \text{the impedance tends to infinity.}$$

In practice the impedance would tend to the equivalent resistance and the component corresponding to this frequency would be uniformly distributed across the coil elements. This is the same as the critical frequency defined before.

For frequencies above the critical frequency the impedance Z is negative, i.e. it is capacitive. The effective capacity of the arrangement is K' and is defined by

$$\begin{aligned} Z &= \frac{1}{j\omega K'} \\ &= \frac{j\omega L}{1 - \omega^2 LK} \end{aligned}$$

$$\text{i.e. } K' = K - \frac{1}{\omega^2 L} \quad \dots\dots\dots (20)$$

This forms the familiar capacitive ladder network considered earlier.

$$\text{Making } g' = \sqrt{\frac{C}{K'}}$$

and substituting into equation 3

$$V_m = V \frac{\text{Sinh}(n-m)g'}{\text{Sinh } ng'} \dots\dots\dots (21)$$

Likewise for frequencies below the critical, the impedance of the parallel element is positive and hence forms an equivalent inductance

$$\begin{aligned} L' &= \frac{L}{1-\omega^2 LK} \\ &= \frac{L}{1-\left(\frac{\omega}{\omega_c}\right)^2} \dots\dots\dots (22) \end{aligned}$$

This forms an inductor-capacitor ladder network which behaves as a transmission line. For frequencies below the critical the coil tends to act as a transmission line.

This has a propagation velocity of

$$\begin{aligned} v' &= \frac{1}{\sqrt{L'C}} \\ &= \sqrt{1-r^2} \dots\dots\dots (23) \end{aligned}$$

where v = propagation velocity without the influence of inter-turn capacity

$$r = \frac{\omega}{\omega_c}$$

Similarly the characteristic surge impedance of the arrangement is

$$z' = \sqrt{\frac{L'}{C}}$$

$$= \frac{z_0}{\sqrt{1-r^2}} \quad \dots \dots \dots (24)$$

where z_0 = surge impedance of the arrangement without the inter-turn capacity present

v' and z' are frequency dependent and tend to v and z_0 when the frequency is low.

This approach is useful when the frequency components of the incoming wave are known. It is often difficult to estimate precisely the frequency components of a steep surge. Wellauer [23] analyses this by considering an impulse having the form of a Sinc integral viz

$$u = \frac{u}{2} + \frac{u}{\pi} \int_0^{\omega t} \frac{\sin \omega t}{\omega} d\omega \quad \dots \dots \dots (25)$$

This yields the shape of impulse shown in figure 3.3

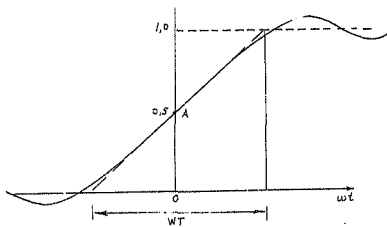


Figure 3.3 Sinc integral shaped impulse

This is assumed to approximate to a normal impulse. It contains all the frequency components from 0 to w . The maximum slope of the impulse is at A and is

$$\frac{du}{dt} = \frac{1}{T} \dots \dots \dots (26)$$

$$\text{i.e. } wT = \pi$$

If the rise time of the impulse is T_s then the maximum frequency components in the impulse are

$$w_{\text{max}} = \frac{\pi}{T_s} \dots \dots \dots (27)$$

This offers an approximate test to see if any components lie above the critical frequency. Those above the critical frequency, w_{cr} , have the form

$$u^{**} = \frac{U}{2} + \frac{U}{\pi} \int_{w_{cr}}^{w_{\text{max}}} \frac{\text{Sin } wt}{w} dw \dots \dots (28)$$

and those below the critical frequency are

$$u^* = \frac{U}{2} + \frac{U}{\pi} \int_0^{w_{cr}} \frac{\text{Sin } wt}{w} dw \dots \dots (29)$$

Wellauer derives the position for the limiting case of a rise time of zero which gives a potential across the first turn of

$$u_{\text{max}} = \frac{U}{T, \pi} \sqrt{\frac{C}{K}} \dots \dots \dots (30)$$

Compare this with equation 8 viz

$$V_0 = U \sqrt{\frac{C}{K}}$$

It is to be noted for the test wave chosen previously i.e. rising at 20 KV/microsecond/KV of rating to 5x rated volts, that the maximum frequency component by this method

is

$$\omega_{\max} = \frac{T_s}{T_s} \text{ where } T_s \text{ is } 0,25 \text{ microseconds}$$

$$\text{i.e. } \omega_{\max} = 1,25 \times 10^7 \text{ radians/sec}$$

Choosing a typical motor coil with $L = 10^{-5}$ H/turn and $K = 400$ pF/turn yields

$$\omega_{cr} = \frac{1}{\sqrt{LK}}$$

$$= 1,6 \times 10^6 \text{ radians/sec}$$

Such a coil could have frequency components above this which do not tend to travel through it and it can be assumed that most coils would tend to behave in a similar fashion as the parameters chosen are realistic ones.

So far the effects of losses and mutual inductances have been ignored. The losses are complex and are frequency dependent. They tend to affect more the higher frequency components of the wave front accentuating the degrading of the wave front with passage through the coil. Rüdénberg [3] considers only the mutual inductance between adjacent turns. He states that this tends to give a critical frequency as before, but modified to

$$\omega_{cr} = \frac{1}{\sqrt{LK - M^2}} \dots \dots \dots (31)$$

where M is the mutual inductance between adjacent turns

The effect of such mutual inductance is thus to raise the critical frequency and allow a higher penetration of high frequency components into the coil. It is assumed that the effects of mutual inductance affect motors less than transformers as the coils are screened by the stator slots from each other. A general solution for a system involving mutual inductances requires the solving of a Fredholm type of integro-differential equation. As this is unsolvable

in closed form an iterative successive approximation solution must be sought involving a computer programme,

In practice most coils appear to have a higher inter-turn capacity than ground capacity due to the symmetry of the coil cross-section. The conductors are closer to each other than to ground and expose more surface area to each other than to ground. This gives a low transfer function, g . For this reason penetration of frequency components above the critical are likely to be relatively deep and no significant change in the entering wave can be expected over the first turn. In these cases a travelling wave model is the simplest and most suitable to use. If the coil has a very low critical frequency then it is wiser to use one of the more complex methods of analysis. Intuitively it can be seen that this would be a rare occurrence as the travelling wave is unlikely to be affected by something right on the boundary of the coil, such as the first turn parameters.

4. TRANSIENT MEASUREMENTS ON COILS USING LOW VOLTAGE SURGES

A practical description of surge behaviour on various coils is attempted. This is done not only to substantiate the information contained in the last chapter, but also to provide a practical test applicable to coils already constructed. As theoretical analysis of coil behaviour is difficult, the application of such a test to sample coils may provide a far simpler answer to questions of surge behaviour in a motor than a mathematical study.

Such a practical test requires a minimum of equipment and consists of injecting low voltage steps into the coil while monitoring the progress of the steps through the coil using a cathode ray oscilloscope as in figure 4.1. A repetitive source of steps is required and it was decided here to use a very fast risetime pulse generator. This provided a one nanosecond risetime pulse lasting a number of microseconds at a repetition rate of approximately 10KH_z . The pulse length chosen was sufficient to allow the display of transient phenomena within the coil, while the repetition rate chosen gave a bright, stable display on the oscilloscope. The step was assumed to approximate to an ideal step, a reasonable assumption considering its rapid rise. To observe fully the rapidly changing nature of the transients within the coil, a high input impedance wideband oscilloscope is required, preferably of 100MH_z band-width. In order to affect the performance of the coil as little as possible the oscilloscope must be provided with high impedance probes of low capacity, so as to avoid loading the coil.

Two types of coils were investigated; model laboratory coils and actual motor coils. The model coils consisted of thin wire suspended in air above a ground plane of aluminium foil. The dimensions were large to allow travelling waves a reasonable time to traverse the coil and hence increase the effective time resolution. The motor coils consisted of coils placed in the stator core of a large H.V. motor, fixed in position, but not yet taped together. This allowed access to the ends of the coils for connection. Full details of coil dimensions and parameters are to be found

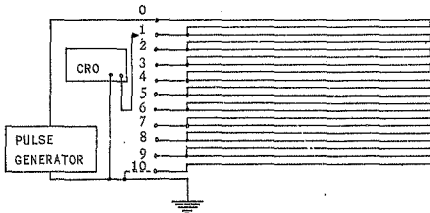


Figure 4.1 Surge measurement on model coil

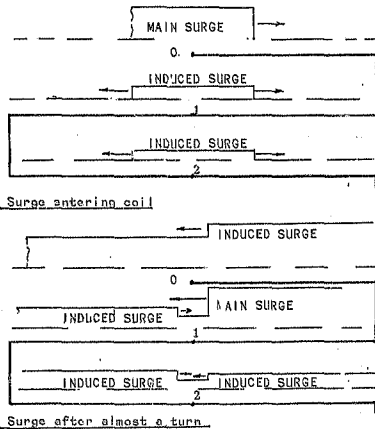


Figure 4.2 Propagation of induced surges on coil

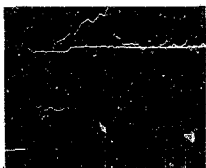
in Appendix C.

4.1 Model Coils - Results

(i) Model coil 1

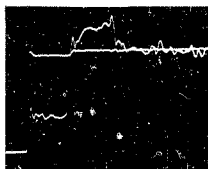
Model coil No. 1 represents a motor coil in layout having 10 turns equidistant from each other and set a fixed distance from earth. The spacing chosen gave a reasonable ratio between turn capacity to earth and capacity turn to earth. The C/K ratio was 0,75 giving a transfer function g of 0,86. This allowed a measurable departure from ideal transmission line behaviour due to inter-turn capacitive coupling. A number of facts were revealed.

- (a) An initial electrostatic distribution of 0.4 of the applied potential was established immediately on the first turn. Oscillograph 1 shows the potential one turn from the start compared to the input of the coil, for an unterminated (open circuited end) coil. The case for a short circuited coil is little different (Oscillograph 2), as would be expected from theory. (Appendix C). The case for the third turn (Oscillograph 3) is however different and emphasises that the original mathematical model was only an approximation for a more complex field arrangement. The initial potential at the third turn should have been 0,2V. This distribution is 0,3V due to the effects of shared fields between capacitive elements of the original model. This is not likely to be so in an actual motor coil, where the conductors are large and flat, tending to screen each other and thereby separating the various capacitive elements and their fields. It does illustrate that a certain amount of the stress across the first turn, present while the travelling wave transverses the coil, is relieved by the electrostatic field arrangement established immediately. The full potential of the impulse is not imposed across the inter-turn insulation of the first turn. The reduction in this stress can be calculated as in Appendix C (In this case 0,43 of full voltage).
- (b) A travelling wave is observed on the coil. This



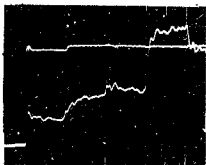
x = 50 ns/div

4.1 Coil 1, V_1 , End o/c



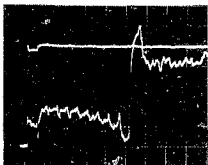
x = 50 ns/div

4.2 Coil 1, V_1 , End s/c



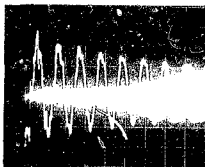
x = 50 ns/div

4.3 Coil 1, V_3 , End s/c



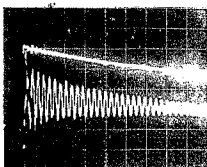
x = 100 ns/div

4.4 Coil 1, V_{10} , End o/c



x = 5 μ s/div

4.5 Coil 1, V_{10} , End o/c



x = 5 μ s/div

4.6 Coil 1, V_5 , End s/c

takes 0,1 microsecond to transverse one turn of 30 metres (1 and 2) and 0,3 microseconds for 3 turns (90 metres) (#3). This yields a propagation velocity of 3×10^8 metres per second, i.e. the velocity of light in an air medium.

- (c) Minor travelling waves are electrostatically induced into the conductors close to the main wave. These travel both forwards and backwards along the coil. The main surge tends to ride over the backward-travelling waves (see Figure 4.2). This explains the apparent overshoot of the main wave observed at point 1 (#1 and #2). The same minor wave travelling forward passes point 2 simultaneously (#3) and is due to the induced potential on turn 2. This backward wave is reflected at the source, which, having a low impedance (50Ω), causes a negative wave to be returned. This explains the abrupt drop in the main wave at point 1 after 0,2 microseconds, (#1) which is due to the returned minor wave arriving at this point. These minor waves can cause small transient overvoltages at various points in the coil. The main effect is that of reflecting energy back towards the source. Oscillograph 4 shows the voltage at the end of the coil (turn No. 10) and it can be seen that about 0,6 of the surge voltage arrives at this point, taking into account the potential doubling of the open circuited end. In Oscillograph 5 taken at the same point over an extended time scale, it can be seen that the electrostatically induced waves eventually begin to predominate. The coil is now resonating with a frequency fixed by its total inductance and inter-turn capacitance. The main wave can still be observed arriving every 2 microseconds until it disappears after approximately 35 microseconds (#5). The waveform becomes smoother until it becomes a damped oscillatory sinusoid. The equivalent circuit explaining this behaviour is shown in figure 4.3.

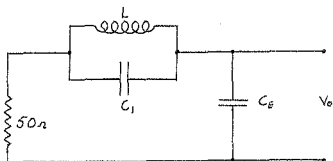
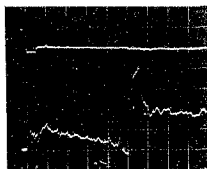


FIG 4.3 EQUIVALENT CIRCUIT

- L = total inductance of coil
 C_1 = internal capacity of the coil turns
 C_E = end capacity of coil to earth

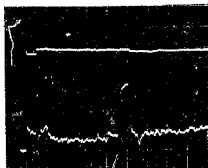
C_1 , in this case, is ignored as it is considered to be ten capacitors (inter-turn) in series and hence rather a low value. On this basis the frequency of oscillation is found to be 184 KHz , which yields $C_E = 250 \text{ pF}$ (see Appendix C), a reasonable figure for the end capacity of the coil turns. Oscillograph 6 shows the potential at the midpoint of the coil with the end short circuited. A similar effect occurs here, with a smooth damped oscillation emerging as the reflected components are eliminated. The oscillation exists between the coil inductance and the inter-turn capacities and is much more rapid. This is due to the reduced capacities involved.

- (d) As the coil behaves as a transmission line it exhibits certain well-known transmission line characteristics. To obtain the surge impedance of the coil its end was terminated by a variable resistance and the effects of varying this termination observed. Oscillograph 7 shows the effect of a 1000 ohms termination.



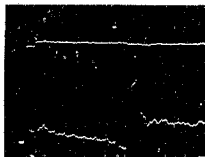
x = 200 ns/div

4.7 Coil 1, V_{10} , 1000 ohms



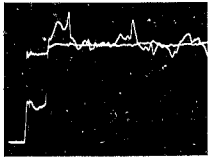
x = 200 ns/div

4.8 Coil 1, V_9 , 300 ohms



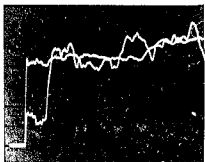
x = 200 ns/div

4.9 Coil 1, V_{10} , 500 ohms



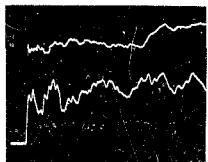
x = 100 ns/div

4.10 Coil 2, V_1 , End o/c



x = 100 ns/div

4.11 Coil 3, V_1 , End s/c



x = 100 ns/div

4.12 Coil 3, V_5 , End s/c

This is too high as a positive surge is retransmitted from the termination and arrives back at the source. This causes a small positive rise in the source waveform after 2 microseconds. This is reflected back as a negative surge arriving back at the termination after 3 microseconds. A value of 300 ohms would appear to cause the complete absorption of the surge (Oscillograph 8). This is deceptive and does not indicate correct termination. The minor wave behind the main surge, which is negative, tends to interact with the main surge in such a way that the main surge, its slightly negative reflection, and the minor wave and reflection all cancel. The termination is actually too low. A termination of 500 ohms would appear to be very nearly correct. (Oscillograph 9). Compare this with the open circuited termination (#4). The main surge is now almost half the open circuited value indicating correct termination. This agrees with the theoretical value derived from the equation

$$Z_c = \sqrt{\frac{L}{C}}$$

where L = inductance per turn

C = turn capacitance to ground

For coil 1 L = 55×10^{-6} Henry

C = 220 pF

$$Z_c = \sqrt{\frac{55 \times 10^{-6}}{220 \times 10^{-12}}}$$

$$= 500 \Omega$$

An interesting point is that although the termination affects the main surge, it appears to have little effect on the minor surge travelling behind it. Also observe that while the main surge is attenuated to 0.6 of its initial value, the minor surge appears to be unattenuated by its passage down the coil. The only explanation of this lies in the additive induction of all minor waves as they travel down

the coil.

- (e) Little loss of steepness occurs in the front of the main surge itself. The surge is attenuated by the reflection of energy due to mutual capacitance (or inductance) as discussed above and swiftly ceases to be important. It is still very significant after only one turn of travel into the coil and for practical purposes may be considered to be unaffected in this region. This allows the calculation of maximum stresses at this point to be simplified to that proposed in the theoretical treatment of the previous chapter, namely a simple travelling wave.

(ii) Model coil 2

The configuration of this coil is different from the first one in that although the dimensions are the same the conductors are arranged vertically instead of horizontally (see Appendix C). As is seen in Oscillograph 10, the behaviour is almost identical to Model Coil 1, tending to confirm that electrostatic behaviour is better explained by a field configuration model than a capacitive model. This coil allows shielding of the upper conductors by the lower, yet behaves in exactly the same manner as the previous coil even though a capacitive model would be made up of capacitors whose ground capacitance C varied with position. In analysing a motor coil, care must be taken to see that little common dielectric is shared between the coil turns before a capacitive analysis is used. In most motor coils capacitive analysis is justified.

(iii) Model coil 3

This coil simulates the behaviour of a double layer coil compared to the previous models which simulated single layer coils. The dimensions are similar to Model Coils 1 and 2 (see Appendix C). Although the potential at point 1 is similar to that obtained at the same point in the other coils (Oscillograph 11) the potential across the layers is markedly different (Oscillograph 12). From this it would appear that half the surge potential is imposed across the insulation layer between coil layers for a considerable period. This is likely to heavily stress the insulation at this

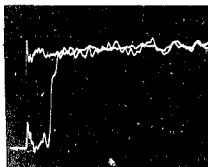
point and a certain amount of over-insulation is indicated. Designers are aware of this and most coils are well insulated at this point.

(iv) Model coil 4

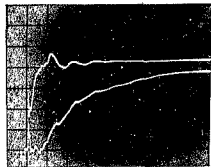
This coil demonstrates the effect of high ground capacity and low inter-turn capacity (see Appendix C). It behaves more as a transmission line than a coil. Observe in Oscillograph 13 the lack of overshoot or initial electrostatically induced potentials, indicating perhaps a link between the two as suggested. Note, also, the decreased velocity of propagation. This is due to the dielectric enamel coating of the wire (Formex) having a far greater share of the ground field than before, due to the proximity of the conductors to ground. The effective permittivity is thus greater than 1.

B. Commercially Produced Motor Coils

The same technique was used on a set of commercial induction motor coils. The coils, wound and insulated, were placed in the stator slots of their motor and wedged in position. The test was performed just prior to the final taping up, allowing access to the bare coil ends. No access was possible to the individual coil turns without damaging the coil insulation so that measurements were conducted purely on inter-coil voltages. (See Appendix C for coil details) Four coils were connected together in series and measurements taken after the first coil. Oscillographs 14 and 15 show the performance at this point with the end of the chain open circuited. Oscillographs 16 and 17 show the performance with a short circuit at the end of the chain. The initial behaviour is virtually the same for both cases ("14 compared to "16). A propagation delay occurs of 0,15 microsecond equivalent to a velocity of propagation of $1,06 \times 10^8$ metres/second. This is equivalent to a wave travelling in a medium of dielectric constant = 7.7. The actual value for the epoxy resin mica ground insulation is between 6 and 9, depending on the material used. A number of internal reflections are discernable at regular intervals. These are reflected versions of the initial electrostatic waves. The driving waveform lacks sharpness due to the increased capacitance of the coil to ground compared to the previous model coil, i.e.



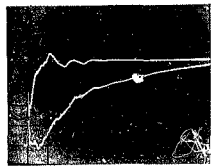
100 ns/div
4.13 Coil 4, V_1 , End s/c



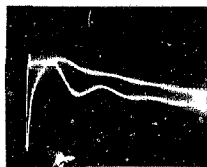
200 ns/div
4.14 Motor Coil, End o/c



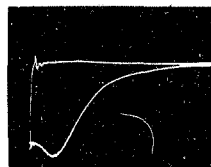
5 μ s/div
4.15 Motor Coil, End o/c



200 ns/div
4.16 Motor Coil, End s/c



2 μ s/div
4.17 Motor Coil End s/c



1 μ s/div
4.18 Motor Coil, 410 ohms

CR=120 nanoseconds, which is in agreement with the measured behaviour. The true behaviour is not this simple as the capacitance is distributed. The capacity presented the first part of the wave is thus effectively low and allows an initial rapid rise to take place before the effects of the entire capacity are felt. The wave is further complicated by minor travelling waves arriving from inside the coil.

A transient of rise-time 250 nanoseconds, in practice, corresponds fairly well to this waveform and is likely to stress the first coil of a winding by an appreciable amount. Considering a 20 KV per microsecond per KV of rating waveform gives approximately 20 KV across the coil. This coil should be tested at 3,3 KV per turn if troublefree operation is desired in an application where sharp surges are likely to be encountered.

It is of interest to note that the attenuation, when the coils are in the motor, is much higher than of air cored coils. This coil, in particular, if provided with an earth of aluminium foil attenuates surges to a much lesser extent than when such an earth is provided by the iron of a stator core. This attenuation is more than likely increased by hysteresis and eddy current losses within the iron of the stator. This is not designed to cope with the high frequencies present in the wave and a high attenuation results.

An anomalous situation exists with a chain of four coils. An open circuited termination leads to an under-damped circuit which oscillates at 73 kHz and has an attenuation factor of $9 \times 10^4 \text{ sec}^{-1}$. Terminating in a short circuit also yields an under-damped circuit, this time of frequency 210 kHz and attenuation factor $3,3 \times 10^5 \text{ sec}^{-1}$. Terminating the end of the coil chain in a resistance tends to increase the apparent damping with a value of 410 ohms giving an apparently critical damping (see oscillograph 18). Assuming a lumped parameter model yields an equivalent circuit as shown in figure 4.4.

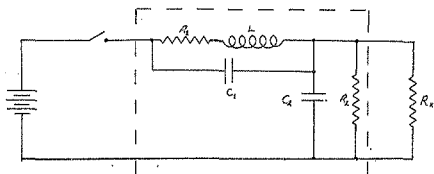


Figure 4.4

- L = Equivalent total series inductance of coils
 C_1 = Equivalent total inter-turn capacitance of coils
 C_2 = Equivalent total ground capacitance of coils
 R_1 = Equivalent total series resistance of coils
 R_2 = Equivalent total shunt resistance of coils
 R_x = External resistance at end of coils

Since the coils are oscillatory at a very much higher frequency when $R_x = 0$, (compared to the case when R_x is infinite), it may be concluded that C_1 is very much smaller than C_2 (by about 10x). Furthermore, even at this high frequency, the value of R_1 is low. In the open circuited case C_1 and R_1 can be ignored leading to a simpler equivalent circuit. Analysing this equivalent circuit yields:-

$$2\pi f_{oc} = \frac{1}{\sqrt{LC_2}}$$

$$LC_2 = \frac{1}{(2\pi f_{oc})^2} \quad \dots \dots \dots (1)$$

Also considering the damping factor α

$$\alpha = \frac{1}{2C_2R_2} \quad \dots \dots \dots (2)$$

Now in the case of critical damping ie when $R_x = 410$ ohms

$$\frac{1}{LC_2} = \frac{1}{(2C_2R)^2} \dots\dots\dots (3)$$

where

$$R = \frac{R_2 R_x}{R_2 + R_x}$$

Knowing R_x , f_{OC} and α , and substituting these values into equations 1, 2 and 3 yields

$$C_2 = 3340 \text{ pF}$$

Also R_2 may be found

$$R_2 = 1660 \text{ ohms}$$

And the inductance L

$$L = 1.44 \times 10^{-3} \text{ H}$$

These values are consistent with the coils acting together, the inductance being that of all four coils plus their mutual inductances. The capacitance is of the same order as that of a single coil to ground.

This reveals an obvious fact, that the coils behave initially like a transmission line which then tends to a highly damped resonant system later on. The later oscillations, being highly damped, constitute little danger to the coil turn insulation. These oscillations are assumed to be evenly distributed across the coils and result in very little stress between actual turns. The initial situation is altogether different. A steep incoming waveform will impose a voltage differential across only the first coil or part thereof resulting in a high stress in this region. The motor tested in this last section may be considered fairly typical; it is significant that even a half microsecond rise-time surge is capable of fully stressing the first coil. As has been seen earlier a certain amount of stress relief is possible by virtue of the

electrostatic distribution within the coil. This merits further study. Such a study is possible only when the coils used are expendable and can thus be penetrated to obtain inter-turn potentials, as in the study on model coils.

5 THE CAPACITIVE DISCHARGE TEST

5.1 INTRODUCTION

One method of testing coil inter-turn insulation consists of discharging a high voltage capacitor through the coil to form an oscillatory underdamped RLC circuit. This leads to an exponentially decaying sinusoidal wave which is imposed across the coil and stresses the inter-turn insulation. The first form of this test was proposed in 1926 by Rylander [29]. The circuit used is that shown in Figure 5.1.

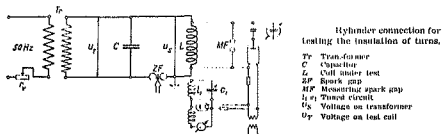


Figure 5.1

A high voltage AC wave from the transformer was imposed across the capacitor, coil, spark gap combination. When the gap broke down, usually near the crest of the AC wave, the capacitor was discharged through the coil producing a damped oscillation. The voltage across the coil was measured using a sphere gap or a peak follower circuit feeding an electrostatic voltmeter. Detection of breakdown was achieved by magnetically coupling another coil and capacitor combination to the test coil and tuning for resonance with a healthy test coil and HV capacitor combination. When breakdown occurred, the change in inductance of the test coil was sufficient to alter the characteristic frequency so that resonance with the sensing coil circuit was lost and a much reduced reading on the meter resulted.

The Rylander method suffered from a number of disadvantages, principally in the detection of breakdown within

the coil. As AC was supplied to the system approximately one hundred impulses a second were imposed across the coil. This could lead to effects not usually found with single impulses, such as damage due to heating or partial discharge phenomena. Breakdown of the spark gap tended to occur at different points on the AC half wave leading to a misleading pulsation of the meter pointer. This could mask an intermittent breakdown within the coil. The most serious defect was no absolute method of detecting a coil failure as the method of detection relied on a sudden relative drop in the meter reading when breakdown occurred. This method would tend to fail to detect a direct short circuit between turns. This event, although unlikely, is possible due to damage in the forming process. Breakdown at very low voltages would also be hard to detect and would allow a coil which was not only potentially faulty, but actually damaged by the test, to be used in a motor winding. A further disadvantage of this detection method was that the reading on the meter was proportional to the coupling between coils and the test voltage, leading to further uncertainty in the meter reading.

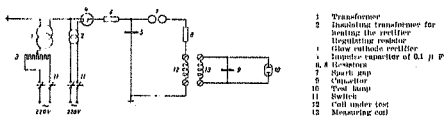


Figure 5.2

Wellauer [32] has attempted to improve the method by using a DC fed capacitor discharged through the test coil. This circuit is illustrated in Figure 5.2 and probably arises from the availability of high voltage rectifiers 15 years after Rylander's original circuit was proposed. It does solve the problem of inconsistent voltages being

applied to the coil. The detection method used is obviously an attempt to a simplified go/no go method, with a neon lamp being used as a voltage detection element. It suffers from all the limitations of Rylander's method with the added disadvantage of not having a continuously graded analogue read out on the detection circuit. An additional feature of Wellauer's method is the inclusion of a damping resistor which causes the circuit to be more damped and hence produces a voltage wave form of the form shown in figure 5.3

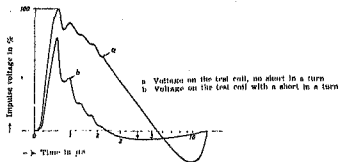


Figure 5.3

Although this waveform is better for coil testing than the underdamped one, personal experience has shown that a large proportion of the capacitor voltage is dropped across the resistor making such a practice inefficient.

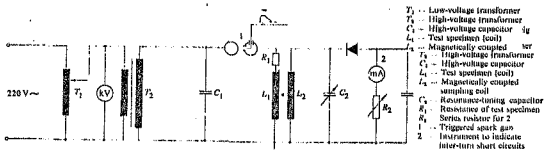


Figure 5.4

Krankel and Schuler [33] have proposed a method which is virtually the same as Rylander's (Figure 5.4). The inconsistent voltages have been overcome by using a triggered spark gap which is operated at the same point on the cycle every time. Their method retains all the other disadvantages of Rylander's method. They test the coils in position in the motor stator which may be rather rash as a failed coil will result in the motor having to be stripped down. They give suitable test voltages (figure 5.5), a feature which other workers have ignored in their articles.

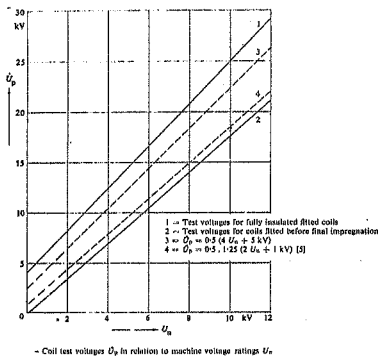


Figure 5.5

They arrive at their values by considering that in practice not more than 50% of surge voltage is likely to be imposed across the entrance coil. They therefore consider a surge voltage to be

$$U_s = 4U_n + 5KV$$

where U_n = normal phase to phase voltage of the motor. Taking 50% of this gives curve 3 in figure 5.5. It can be

seen that the values used are high and coils tested on this basis are likely to be sound in practice. It is noticed that these values are based on the motor voltage only. A more accurate value would have been based on the actual coil characteristics. Coils having a small number of turns would be unnecessarily stressed using the values shown.

A number of workers have used indirect means of testing coils which have already been installed in machine windings. Such methods are useful for testing machines which are already in service. The difficulty here lies in obtaining an adequate voltage across the coil without imposing a high voltage across the entire winding, a situation which can damage the ground insulation. The usual way of achieving this is to induce a high voltage into the coil using an external coil magnetically linked, via an iron armature piece, to the coil concerned.

Oliver et al [1] have used this method to test the inter-turn insulation of large hydro-generators. They detect breakdown by direct examination of the induced waveform with an oscilloscope. Due to the high inductances, frequencies tended to be low, typically 10 000Hz. The apparatus is shown in Figure 5.6. They give no indication of how they obtained suitable test voltage values, but the voltages used were sufficient to breakdown some of the windings tested. They presumed that the waveforms obtained at low surge voltages were indicative of soundness and obtaining a different wave form at higher voltages indicated that a breakdown had occurred.

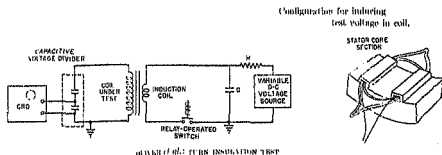


Figure 5.6

A somewhat similar test was used by Sexton and Alke to detect faulty turbo-generator windings [34]. They also used an induced method to obtain high coil voltages, but refined the breakdown detection by using a surge comparison method. This allows the coil under test to be compared with another coil in the winding. An unsound coil will give a different display to the rest of the coils in the winding. A weak point in their apparatus was the use of thyratrons to control the discharging of the capacitors through various coils. As thyratrons are easily damaged by currents higher than the design limits, a resistance was incorporated in series with the thyatron which tended to limit the voltage induced into the coil.

A number of workers have used surge comparison methods to test motors as well. Catlin and Rohats [35] used an Ignitron controlled circuit, but found a large volt drop in the leads to the commutator. Comparison was done by tapping across the commutator bars and comparing voltage wave forms obtained between adjacent bars. Moses and Harter (36) have a method whereby the connections to the winding are alternatively reversed by a mechanical switch. An oscilloscope is connected to the midpoint of the winding and the alternative surges appear displayed as potentials above ground. Reynold's method [37] is similar but employs inducing coils.

The methods described have also been used on low powered, utilitarian type motors, where automatic testing methods are indicated. Weed [38] has developed an electronic tester with an ingenious method of comparing surges in different coils. Capacitors are discharged simultaneously through different coils in the winding and displayed on X and Y plates of an oscilloscope. A Lissouja's figure results. If both coils are sound then a regular figure results, the form usually being a spiral. Should they be different then an irregular figure appears. Strain [39] also describes a surge comparison tester for fractional horsepower motors. His article is helpful in establishing a statistical basis for such tests assuming a 0.1% rejection rate.

5.2 A PRACTICAL CAPACITIVE DISCHARGE TEST

A fact disclosed by careful study of the above references is that few workers have chosen to test coils before they are installed in the motor. Most of them test only the completed motor winding. The only worker obviously testing before installation is Wellauer [32]. Testing before installation has the advantage that any defective coils are rejected before they are installed in the motor. This eliminates having to strip the motor when defective coils are discovered later in the manufacturing process. The disadvantage of testing before installation is that if a coil should be damaged when being installed in the motor, then this damage is unlikely to be detected unless further tests are done later on.

To assess the right stage at which to test the coils requires a knowledge of what faults are likely to occur in the coil inter-turn insulation. The most common faults are those likely to occur during manufacture of the coil.

These include:-

1. Voids in the insulating material due to air bubbles, tears or discontinuities in the insulating material.
2. Foreign matter occluded in the insulation. This includes water, dirt or metallic particles.
3. Sharp discontinuities on the conductors which pierce the insulation. These are usually burrs raised by one of the mechanical processes involved in manufacturing and winding the coils.
4. Cracks in the insulation caused by the pulling of the coils to form the final coil shape.

Damage to the coil during installation in the stator is most likely to be due to excessive physical deformation of the coil. Any such damage is likely to be accompanied by damage to the ground insulation as well. If this is the case then the motor will fail any subsequent corona or pressure test, such tests being normally done before the motor is delivered.

This justifies testing the inter-turn insulation of coils just before they are installed in the stator of the machine. This means that the individual coils have been wound, pulled and finally cured (usually by heat) before being tested.

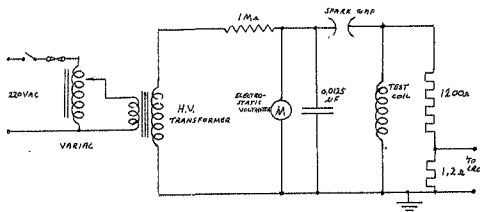
Such coils have low inductances, of the order of 50 to 200 microHenries and require special testing circuits to stress the turns adequately. Due to the inconsistencies of Rylander's method it was decided to adopt a method similar to Wellauer's method. A variable AC supply is rectified and fed to a capacitor. The capacitor is discharged through the test coil via an air gap forming a damped RLC circuit.

The original capacitors employed for this test were those constructed by J.J. Kritzinger for his impulse generator [40]. These consisted of 50 two microFarad paper capacitors connected in series and sealed in a container of insulating grease (Penetroil). They gave a nominal capacity of 0,05 microFarads and a total working voltage of 100 KV. These same capacitors had been used by Jones for his tests on motor coils using the capacitor discharge method [41]. These capacitors gave poor results and it was found subsequently that they presented a very high internal inductance due to the combined effects of the capacitors in series. This inductance was of the order of 10 to 20 microhenries and caused a large proportion of the capacitor voltage to be dropped internally when the capacitor was discharged. Coupled with this was the large physical size of the capacitor which necessitated long leads to be used for connection. It was found that the inductance of these leads added appreciably to the stray inductance present. It was also found that Kritzinger had installed a low resistance in the tube joining the capacitor to its attached discharge sphere. This also caused an appreciable volt drop and had to be removed. As Jones had conducted his experiments with certain of these impediments present, it is doubtful whether his test voltages were anywhere near as high as expected. This indicated that a means of measuring the actual voltage on the coil is required. Such voltages are easily measured by connecting a non-conductive resistive divider across the coil.

To avoid the volt drop due to the high internal inductance of the capacitor, it was decided to search for more suitable capacitors. These were eventually found in the form of ceramic encased capacitors of Admiralty pattern, probably scrapped from a radio transmitter. Although of lower capacity, 0.0125 μ F, and lower rated voltage, 30 KV, they had a very low internal impedance. Their physical dimensions were very much smaller, allowing test coils to be connected directly to the capacitor terminals. This allowed the entire test arrangement, coil, capacitor, shunt resistor and sphere gap to be placed on a tabletop. The close proximity of the components cut down stray inductances to the minimum and ensured that full voltage appeared across the coil.

The sphere gap used had 7.5 cm copper spheres mounted on an adjustment screw which could be turned, via an insulating rod, to change the gap, and hence the breakdown voltage. This feature allowed the test voltage to be changed without de-energising the circuit. It was found unnecessary to use a triggered spark gap as the natural breakdown of a plain sphere gap was consistent and provided an accurately controllable test voltage. Experiments with triggered gaps revealed that they tended to interfere with the CRO used to study the oscillation.

Jones complained of high capacitor leakage currents limiting the value of voltage to which he could charge the capacitor. It was found that the leakage of the capacitor was not causing this effect. The trouble was traced to poor rectifier diodes with excessive leakage. These rectifiers, of the selenium pencil type, were replaced by modern silicon avalanche type. These were capable of passing 0.5 A and avalanched at 22.5 KV. Four of these rectifiers each intended for normal working at 10 KV, were connected in series. This allowed voltages of up to 40 KV to be generated. It was found in practice that the capacitors used were capable of withstanding this voltage despite their nominal 30 KV rating.

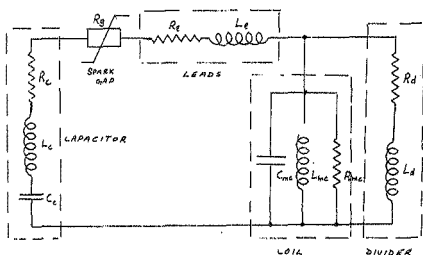


Impulse generator

Figure 5.7

The final test circuit is shown in figure 5.7. Note that measurements are taken from a voltage sensing point, Jones took samples from a current sensing series resistance. It was found in practice that this tended to suffer severely from interference. The arrangement shown tended to place full capacitor voltage across the coil and the advantage was that the voltage displayed on the electrostatic voltmeter was the peak value of that placed on the coil. Thus it was unnecessary to keep referring to the C.R.O. trace to obtain the coil test voltage.

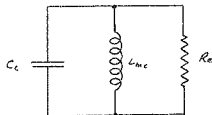
Great care must be taken to ensure that all connectors have as great a cross section as possible to keep down their inductance and reduce the inductive drops in the circuit so as to avoid placing undue voltage stress between the measuring instruments and earth. The earthing point must be placed right at the junction of the coil end and the lower end of the divider. Early tests did not do this rigorously and allowed some alarming flashovers to occur in the C.R.O. connected to the divider. It is obvious that such a situation is dangerous to operators as well as to equipment.



Equivalent circuit of impulse generator

Figure 5.8

Analysing the circuit involved in the discharge yields the complex circuit shown in figure 5.8. This circuit is easily simplified provided due care has been taken to minimise stray inductances and resistances. Choice of a suitable capacitor eliminates the capacitor stray inductance and resistance, L_c & R_c . The air gap constitutes a non-linear resistor, R_g . This may be eliminated as it is only effective before breakdown and at low currents. Inductance and resistance of the leads, L_l and R_l , are assumed negligible. The inter-turn capacity of the coil, C_{mc} , is assumed insignificant compared with the main capacitor, with which it is effectively in parallel. The inductance of the divider, L_d is minimised by the use of non-inductive asbestos based resistive tape. By lumping the divider resistance, R_d with the effective coil resistance, R_{mc} , an effective resistance of R is obtained in the circuit shown in figure 5.9. An analysis of this simple circuit is presented in Appendix C.

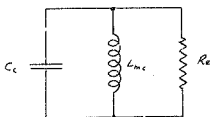


Simplified equivalent circuit

Figure 5.9

The circuit analysis is useful for the initial design of the test circuits, allowing a rough choice of capacity and divider resistance. The final choice of such components rests in direct experimentation as the coil inductance and resistance depend on skin effects within the coil due to the high frequency fundamental component of the test waveform. This skin effect depends on conductor size and configuration and is difficult to predict theoretically, justifying such a practical approach.

Previous workers have not indicated any standard waveform for this test. This is a serious omission as different fundamental frequencies and decay rates could have an effect on the test results. This applies especially to the amount of stress imposed across initial turns. A lower frequency also implies the use of a larger capacitor which means that a larger amount of stored energy must be dissipated when this is discharged. It is useful to compare this test with the standard impulse test, specified by I.E.C. specification 50 [10]. This specifies a standard impulse waveform with an impulse rising in voltage to the crest value in 1.25 microseconds and decaying in 50 microseconds as shown in figure 5.10 (a). Specifications such as this one, allow constant impulse testing of electrical equipment.



Simplified equivalent circuit

Figure 5.9

The circuit analysis is useful for the initial design of the test circuits, allowing a rough choice of capacity and divider resistance. The final choice of such components rests in direct experimentation as the coil inductance and resistance depend on skin effects within the coil due to the high frequency fundamental component of the test waveform. This skin effect depends on conductor size and configuration and is difficult to predict theoretically, justifying such a practical approach.

Previous workers have not indicated any standard waveform for this test. This is a serious omission: different fundamental frequencies and decay rates could have an effect on the test results. This applies especially to the amount of stress imposed across initial turns. A lower frequency also implies the use of a larger capacitor which means that a larger amount of stored energy must be dissipated when this is discharged. It is useful to compare this test with the standard impulse test, specified by I.E.C. specification 50 [10]. This specifies a standard impulse waveform with an impulse rising in voltage to the crest value in 1.25 microseconds and decaying in 50 microseconds as shown in Figure 5.10 (a). Specifications such as this one, allow constant impulse testing of electrical equipment.

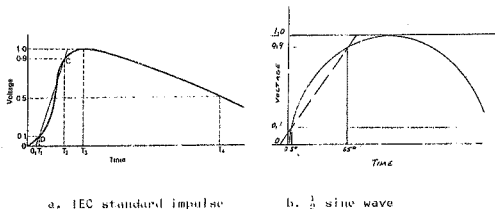


Figure 5.10

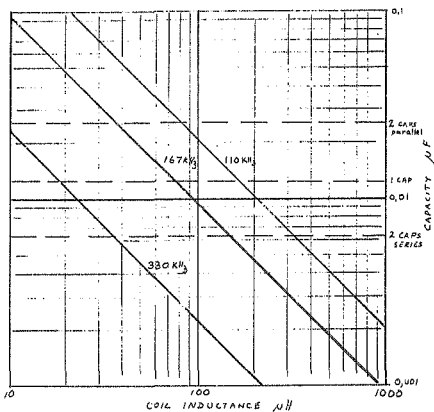
A standard waveform for capacitive discharge testing could conveniently be based on this standard waveform. This allows a decay of the envelope of the damped oscillation to follow that of the standard $1.25/50$ waveform i.e. decaying from peak voltage, V_p , to half this voltage, $\frac{1}{2}V_p$, in 50 microseconds. The basic frequency of the oscillation is selected to correspond with the rise time of the standard wave i.e. 1.25 microseconds. The method of calculation is shown in figure 5.10 (b) which is similar to that adopted with the standard impulse. The 10% to 90% portion of a sine wave corresponds to 60° as shown. Thus the total rise corresponding to the straight line through these points is achieved in 75° of a wave of frequency f . As one cycle is 360° this corresponds in time to

$$\frac{75}{360} \approx \frac{1}{f}$$

which must be 1.25 microseconds. This yields f as 167 KHz. The impulse specification allows a 50% tolerance on this figure i.e. acceptable frequencies from 330 KHz down to 110 KHz approximately. This allows frequencies in the range 150 to 200 KHz to be perfectly acceptable. The tolerance on the envelope decay is 20% i.e. 40 to 60 microseconds.

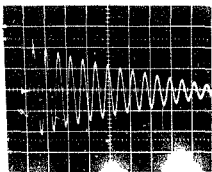
The preferred method of achieving this standard waveform is by first selecting the capacitor or capacitor combination which will give the correct frequency. This should

give a wave which is sufficiently underdamped to have an envelope decay slower than the standard one. Adjustment of the value of the shunt resistor used to monitor voltage allows the exact decay to be achieved. Such a procedure resulted in the waveform shown in photograph 1. Selection of the correct capacitor combination with a coil of a certain inductance may be ascertained from Figure 5.11.



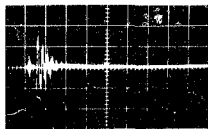
L-C combinations for allowable impulse frequencies

Figure 5.11



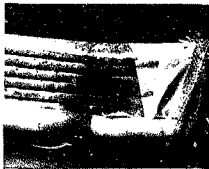
X: 10 μ s/div Y: 5 KV/div

5.1 Sound coil waveform

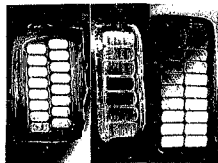


X: 10 μ s/div Y: 5 KV/div

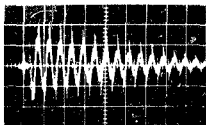
5.2 Breakdown waveform



5.3 Discharge track

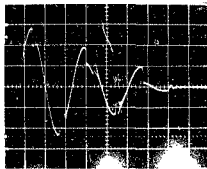


5.4 Coil Sections



X 10 μ s/div

5.5 Current waveform



X 5 μ s/div Y: 500V/div

5.6 End of discharge

5.3 DETECTION OF BREAKDOWN IN THE CAPACITIVE DISCHARGE TEST

The most difficult aspect of the test is the detection of any breakdowns between turns of the test coil. As stated before, previous workers have mostly used a tuned secondary coil. This is designed to resonate at the same frequency as the healthy coil capacitor combination. Potentials induced magnetically in it are rectified and fed to a meter. If the coil should break down, the frequency of oscillation changes, reducing the induced voltage, and hence the reading on the meter.

The method has a number of disadvantages. The resonant circuit must be adjusted for each new set of coils if these are of differing inductance. It may even be necessary to adjust for each separate coil. Voltage must be applied in gradually increasing steps; breakdown being indicated by a sudden drop in the meter reading. Thus the meter reading is relative and is tied to the test voltage. Obviously with this method it is not possible to determine absolutely whether or not breakdown has occurred without some sort of reference. In most cases this reference is the test coil itself at a lower voltage. Another standard coil which is known to be sound may also be used as a reference. In this case both coils must be identical.

A number of methods have been tried in an attempt to find a reliable means of indicating breakdown. The most commonly used method in the tests done was to monitor the voltage across the coil, via the potential divider, using a cathode ray oscilloscope. It was found that the waveforms given by sound and unsound coils differed so markedly that positive identification by this method is assured. This may be observed by comparing photograph 1, (a sound coil), with photograph 2 (an unsound coil). Photograph 2 shows a waveform which is not only of higher frequency, but also of greater attenuation. It also appears far more complex with noise and high frequency components superimposed on the fundamental wave. This wave appears different from the sound one because the breakdown appears to absorb a large amount of energy whilst at the same time effectively reducing the inductance of the coil.

The short circuited elements of the coil also tend to oscillate, producing complex high frequency waves. The breakdown discharge causes noise to be generated in the circuit. All this leads to a highly distinctive waveform. Previous workers have noted that breakdown is difficult to detect using this method. In these cases the machines tested were often large generators with the coils already installed in the stator. It can only be surmised that the effects of the stator masked the breakdown effects. As can be seen in Chapter 4, this leads to considerable attenuation due to the iron of the stator damping out high frequencies. This iron is designed to have a low loss at low frequencies only. Coil geometries are also important. It was found that most discharges within the motor coils did not tend to take place between adjacent turns, but rather between a number of turns (see later). This accentuated the drop in inductance as well as allowing more voltage and energy to be absorbed by the fault. Obviously the lower the stray inductance of the circuit, the more noticeable this effect becomes. If one is forced to discharge through a series of coils in a winding then the effect of one turn on a coil going short could easily be missed. It is not known whether more than one turn would tend to be involved when a large generator, with its differing coil geometries, is tested. Despite the findings of other workers, it is felt that although this is not entirely an absolute fault detection, it is still the most useful. It is recommended for any laboratory tests as more information than is gained from determining breakdowns is gained from it.

If one wishes to avoid using an oscilloscope then other methods of breakdown detection may be used. This may be required when testing in a factory environment using semi-skilled labour. Jones [41] discovered that an electronic counter connected to the current sensing output gave an indication of breakdown by the number of counts registered on the counter. The counter was operated in the manual mode i.e. it remained activated by a pushbutton during the test and counted all crossings of a preset trigger level. No indication of the actual trigger level is given. The drawback

with this method is that the count varies with trigger level and with test voltages. Jones found that he obtained counts of about 25 with sound coils and 8 or 9 with failed coils (typically). He surmised correctly that this was due to the much higher rate of decay of the failed coil wave. This allows less oscillatory wave crests to exceed the trigger level and be counted.

It was decided to improve on this means of detection using equipment that was simple to operate and economical to purchase or construct. It was found that none of the counters available in the Electrical Engineering Department were suitable for this purpose. It was decided that a custom built counter unit offered the best solution to this problem. Such a counter employing TTL integrated circuitry, was designed and constructed. The circuit of this counter is shown in figure 5.12. The signal from the voltage divider, in this case 1:1000, is fed to attenuators. The attenuators have zener diodes to limit the voltage and to remove negative half wave signals. Both attenuators feed 74121 monostable multivibrators via their Schmitt Trigger inputs. These are designed to operate at 1.5 volts positive going levels. The less sensitive input (high attenuation) multivibrator controls the operation of counting and latching circuit. On receiving the impulse, this monostable starts a timing cycle which is designed to be as long as the impulse decay. The output of the monostable places a low input on the reset of the two decade counters, type 7490. This enables them and allows them to count. At the same time a high is placed on the enable input of the latches allowing the output of the latch to follow its input which is the BCD output of the decade counters. The latches feed BCD to seven segment decoders which drive seven segment incandescent displays.

The more sensitive attenuator drives another monostable giving pulses corresponding to the positive crossings of the 1.5 volt level by the impulse wave. The pulses feed into the first decade counter which counts them feeding ten pulses to the next counter. At the end of the cycle determined by the first monostable time delay the decade counters are reset to zero. Simultaneously a signal is sent which locks the

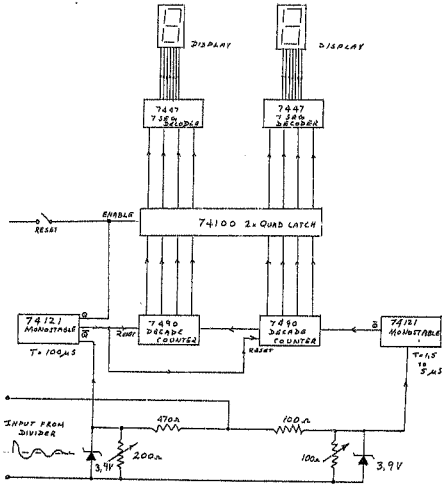


Fig. 5.12 Specialised counter for breakdown detection

latch preserving the BCD output of the counters before they are reset. This method avoids having to reset the counters manually each time.

The refinements in this circuit lie in the correct adjustment of the monostable circuits. The first monostable is designed to be triggered only once by the impulse waveform, its input being below the trigger voltage at the end of one timing cycle. The timing period can be adjusted to be longer than the impulse decay period or shorter. If the counters are still being fed at the end of the timing cycle, then a consistent number of counts are obtained regardless of test voltage. Allowing a fairly unlimited period for this allows more counts to be recorded at higher test voltages. The period of the second monostable has an important effect on the detection of breakdown. The period of the pulses produced are adjusted so that they allow the monostable to reset in time to catch the following positive half cycle in the impulse. Should breakdown occur then the frequency increases and the monostable, being activated, misses those half-cycles arriving within the pulse. This reduces drastically the number of pulses likely to be counted when breakdown occurs. In addition, the faster rate of decay of the impulse allows less half cycles to exceed the trigger level.

The detector was tested with the attenuators both set to their most sensitive setting, with the time cycle set to 110 microseconds and the pulse length to 3 microseconds. The wave form shown in photograph 1 was applied and for all test voltages gave a consistent count of 20. When the coil was faulted to produce the wave form of photograph 2, the count dropped to 1, occasionally 2. Tests on other coils confirmed these figures and allowed a powerful discrimination of sound and unsound coils.

The detector is simple to set up. With the test coil in position, a low voltage impulse is applied. (A value of 5 K V is suggested). The timing attenuator, A, is adjusted so that the monostable is just activated allowing a count to be registered. This can be seen when the display operates after having been set to zero by the manual reset button. The timing monostable is then adjusted to obtain a

convenient count, usually 20. The other monostable (B) is then adjusted to give pulses just narrower than the impulse oscillation period. This is done by increasing the pulse period until the count suddenly drops to half its previous value. The adjustment is then hacked off by a convenient amount, usually just enough to give full count. Test voltages may now be applied.

This detection method still has the disadvantage that a comparison must be made between an assumed sound coil and the tested coil, in this case the sound coil being the test coil at a lower voltage. Care must also be taken with this detector that it is adequately screened and supplied from an interference-free DC supply, otherwise interfering signals from the H.V. circuitry will cause trouble. A further refinement to the circuit was contemplated but never attempted. This was to allow a delay of a few microseconds in the enabling of the counters to avoid recording any of the pulses due to a broken down coil. A sound coil would give a full count as usual. It was also thought possible to eliminate the decoders and readouts by having a simple go/no go system whereby a count of more than 10, say, would cause a light to operate. This would allow the use of only one counter and a bistable multivibrator, instead of the digital elements shown. (see figure 5.13)

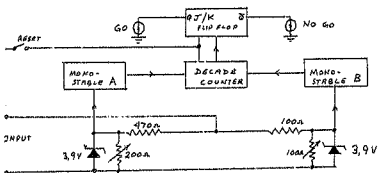


Figure 5.13 Go/No go counter

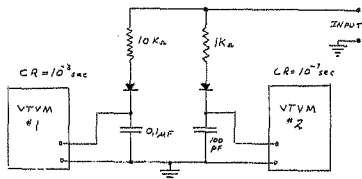


Figure 5.14 Simple detector

Another simple method of detecting breakdown used the circuit shown in Figure 5.14. This consists of two sections, each section having a capacitor charged through a resistor by a rectified version of the impulse wave derived from the voltage divider. The final voltage across each capacitor is sensed by a high impedance electronic voltmeter. Section 1 has a short time constant, 10^{-7} second, and works as a peak detector. It allows the voltmeter to record the full voltage of the impulse. The other section gives an approximately integrated version of the half wave, as it has a long time constant, 10^{-3} second. A sound coil when tested gives a large value of time integrated voltage. When the coil breaks down this drops and a very much lower voltage is recorded by its voltmeter. This method of use of the circuit relies on both meters reading the same amount when the coil is sound. This can be arranged by adjustment of the meter sensitivity and the resistance feeding the integrating capacitor using a low test voltage. Both meters will now give roughly the same indication, rising with an increase in test voltage, until breakdown occurs when the integrating meter drops to a very much lower value, and the peak detector remains almost the same.

Breakdown may also be detected by the differing sound

given off by the test setup. A louder, sharper crack usually results. However, this means of detection is far too empirical and unreliable. It is also possible to observe the discharge directly in some cases. A red flash can be observed on the ends of the coils if they are wrapped with glass tape insulation.

5.4 AN IMPROVED TEST SUITABLE FOR FACTORY USE.

The capacitive discharge test described earlier has a number of drawbacks limiting its use as a routine testing procedure in a factory environment.

These are:-

1. Lack of any definite absolute method of detecting breakdown.
2. Potential physical danger to test personnel. This is unavoidable due to the use of a dangerous charged capacitor as well as the direct handling of metallic contacts.
3. Changes in coil types lead to changes in impulse frequency and attenuation. This leads to setting up delays and expenses every time a new type of coil is tested.

To overcome these problems an induced impulse method is proposed. This method uses a capacitor which is discharged through a fixed coil which acts as the primary of an air cored transformer, the secondary being the test coil. In this way the frequency and attenuation of the impulse is controlled mainly by the capacitor and primary coil and not to any large extent by the test coil. Thus a large variety of test coils may be impulsed without the induced impulse exceeding the tolerances specified for basic frequency and attenuation. The test coil may be galvanically separated from the circuit containing the capacitor.

Such a circuit has the drawback that induced voltages are highly dependent on the coupling between coils. A voltage measuring system is required, which can be attached to the test coil. To lessen the effect of this measurement on the primary circuit, it is preferable that this instrument have a high impedance. As the system could be designed for go/no go conditions, a spark gap was decided upon. The spark gap, set for the test value, breaks down when the test voltage reaches this correct value. The test voltage is achieved by raising the capacitor discharge voltage in the primary circuit by steps until the spark gap breaks over on the secondary.

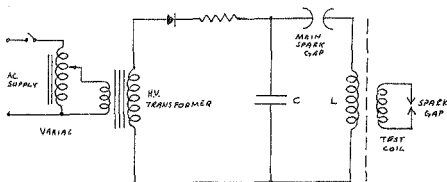


Figure 5.15 Practical production tester

The circuit to conduct this test is shown in Figure 5.15. It is very similar to the ordinary capacitive discharge tests. The primary circuit is placed in a closed cubicle with the coil arranged to couple with the test coil in an upper separate cubicle which can be opened by the operator. The floor of the upper cubicle is of insulating material and separates the two coils, allowance being made for them to be sufficiently isolated from each other electrostatically, but with a large degree of magnetic coupling. The door to the test cubicle controls the power to the test circuit as well as placing a bleeder resistor across the capacitor. The ends of the test coil are inserted in cups which lead to the spark gap. The spark gap is fully adjustable to allow any voltage to be used. It is calibrated directly in volts. As a further precaution, the coil under test may be handled only with gloves and by its ground insulation.

Should an internal breakdown occur during the test then the voltage in the test coil collapses and it becomes impossible to achieve a breakdown of the spark gap. The arrangement shown in Figure 5.15 was constructed and tested with a number of coils known to be sound and faulty. It was discovered that sound coils easily achieve test voltages provided they were reasonably coupled to the primary coil. Faulty coils displayed very low voltages across their ends as well as causing considerable damping on the primary wave. This method also has the advantage of providing virtually

the same amount of volts per turn regardless of the number of turns in a coil. This allows a much larger variety of coils to be tested, as with the other test the full coil voltage required must be placed virtually on the capacitor. Sometimes with multi-turn coils this voltage can be excessively high due to the large number of turns on the test coil. With the induced test method the test voltage is automatically increased to accommodate this without having to increase the capacitor voltage.

5.6 STATISTICAL TESTS ON THE CAPACITOR DISCHARGE METHOD

Before the capacitor discharge method can be used for production testing of motor coils, a number of facts must be known about the tests.

1. Does the test tend to stress different turns of the coil unevenly? This is of importance when winding the motor as coils must then be inserted into the stator with the same orientation as that used when testing the coil. Failing this, coils must be tested on the basis of the lowest turn to turn voltage. This means that the areas displaying high turn to turn voltage will be overstressed leading to a high coil failure rate during the test.
2. Is the inter-turn insulating material weakened in any way by the test? Should the test cause damage to the insulation then it is of little use for production testing. Such damage may be due to chemical changes, mechanical effects or partial discharges, or a combination of these.
3. How does the test relate to the standard method of impulse testing? This method employs the standard impulse (1.25/50) on dissected coils as detailed earlier.

The answers to these questions can only be given by a full statistical study of the test using a large number of motor coils. Unfortunately such an exercise would prove extremely costly due to the high production cost of high voltage motor coils. Such coils, besides containing a fair amount of copper and expensive insulating material, also use a large amount of labour, as the taping is usually done by hand. Such a test procedure is only within the resources of a large manufacturer and even then may be considered too expensive to justify. Furthermore, difficulty can be expected in producing a large number of completely identical coils. Tests using actual motor coils are thus impossible in a low budget project such as this.

A limited number of coils are available from manufacturers and commercial motor rewinders. These are spare coils

over at the end of a motor winding job. When a large motor is wound, more coils than necessary are produced. Should a coil be damaged during insertion or testing then a replacement is readily available from these extra coils. The number of such coils redundant at the end of a job is kept as low as possible, due to their high cost. It is unusual for more than one or two coils to remain over. Such coils are salvaged where possible and, if the motor is a standard item, they are held in stock until the next motor employing the particular coil is required. Non-standard motor coils are usually scrapped and it is such coils which may become available. Obviously such a source yields coils which are of varied types and few in number. As such these coils are unsuitable for a direct statistical test programme.

The significant fact about testing a complete coil is that breakdown only occurs in one small portion of the inter-turn insulation. If one could replace this portion of insulating material then the same coil could be tested over and over. This would provide an answer to both questions 1 and 2 above.

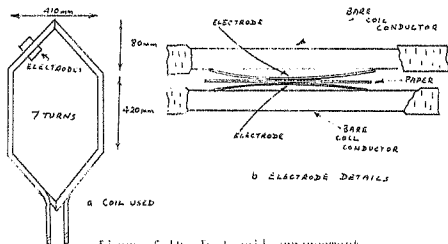


Figure 5.10 Test coil arrangement

A sturdy, well insulated motor coil was selected from those available (see figure 5.16). The first turn was split in the position shown and two copper plates inserted. These plates acted as electrodes with the turn potential across them. They were carefully polished and maintained in a smooth condition to ensure consistent contact with any samples between them. The coil was used in a capacitive discharge test configuration as in figure 5.7. It gave a healthy discharge as shown in photograph 1. The coil was placed on a wooden table one metre above ground level in a horizontal position, with the capacitor and sphere gap next to it. The split turn was conveniently exposed for insertion of samples.

The samples used should by rights be actual samples of inter-turn insulation material. Unfortunately such samples are difficult to obtain and use. The material used usually consists of an enamel layer on the conductor followed by a layer (or layers) of glass fibres impregnated with an artificial resin. A true sample of such a material must be stripped from a conductor and flattened before being tested. This would severely damage the sample. The ideal material for these tests must be readily obtainable in flat uniform sheets and should preferably be electrically fragile. It was eventually decided to use paper, with due care being taken to ensure a consistent quality of samples. The paper used was a photocopying paper produced by the 3M Company. It is a high quality paper with a xerographic coating. Such paper has a high resistance to enable the electrostatic image to be retained. A sample of this material is provided.

The samples used were taken from the centre of a stack of paper and handled only by the edges with clean hands. It was presumed that only the centre of the paper could be considered clean and a strip 25mm wide was removed from all sides when the samples were cut. This was done using a photographic quillotine and the samples were cut in such a manner that they dropped straight into a polythene bowl without being handled. Samples approximately of 50mm x 100mm were prepared. A much larger number than that required was prepared. The samples were then mixed by placing a cover on the bowl and shaking it. The open bowl was placed in a

PAPER SAMPLE

cool dry place and covered with a dry cloth to exclude dust. The mixing procedure was repeated vigorously once a day for a week. At the end of this period the samples were considered to have normalised the weather having been consistently dry during this period.

During the tests samples were removed at random from the covered bowl. This was done one at a time using tweezers to grip the paper at the corner. This was placed between the electrodes which were under a slight compression due to their shape and the natural springiness of the coil turns. It was established at the start that samples had breakdown values of about 6 KV or higher measured over the entire coil. The tests therefore began at 6 KV. Two discharges at approximately 10 second intervals were imposed on the sample. The voltage was raised by 500 volts and the procedure repeated, 30 seconds later. The potential of the discharge was raised in this manner until breakdown occurred. The breakdown was directly visible between the electrodes.

Five different test configurations were used. Each day for five days, ten samples were tested on each configuration and the tests were done in a different sequence on different days. The temperature remained between 18°C and 20°C during all the tests. After each of the group of ten breakdowns per configuration, the electrodes were repolished to establish the same conditions for the next group of tests. A number of samples with deliberately introduced holes were also tested to establish the breakdown of an air gap of the same separation as the thickness of the paper. It was found that this gave breakdowns at a maximum of 3 KV, half of the lowest value with the paper in position.

The tests done were:-

test 1 The coil was arranged so that it presented the first turn to the sample. The capacity to earth was minimised by having as few 'earthy' objects as possible close to the coil.

Capacity to earth 22pF

Inductance of coil 63 microhenries

test 2 Similar to test 1 but with coil arranged to present last turn to sample.

Test 3 First turn presented to sample, with an aluminium foil earth screen placed around the straight portions of the coil to simulate the effect of the stator. This was connected directly to circuit earth.

Capacity to earth = 155pF

Inductance of coil = 0.2 microhenries

Test 4 Similar to test 3 but with coils arranged to present last turn to sample

Test 5 The same as test 1, but the sample was discharged 25 times at 0 kV at 10 second intervals prior to being tested in the usual manner.

The results are summarised here. A more detailed presentation is available in the histograms Figures 5.17 and 5.18

Test	Average breakdown (KV)	Standard deviation
1	7.84	0.45
2	8.04	0.45
3	7.08	0.50
4	7.58	0.41
5	7.80	0.43

Number of samples = 20

Tests 1 and 2 give results which are within 2.5% indicating that there is little difference between first and last turns when the earth capacity is low.

Tests 3 and 4 give results that are within 0.7% indicating the influence of the increased earth capacity on the dissimilarity between breakdowns of first and last turns. The explanation is available to account for the drop in overall breakdown voltage between this configuration and that of tests 1 and 2.

Comparing test 5 with test 1 indicates that repeated stressing of the samples at 75 to 80% of the average break-

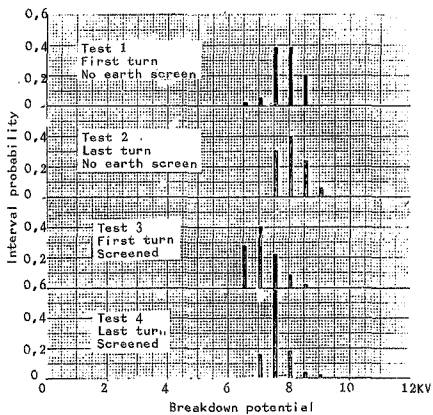


Figure 5.17 Histograms of initial turn breakdown tests

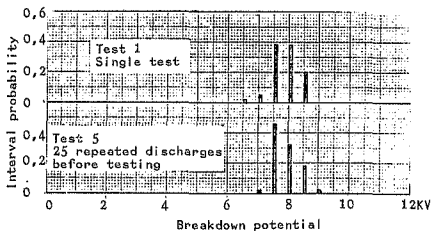


Figure 5.18 Histogram of repeated discharge test

d wn voltage does not appear to lower the breakdown voltage of the samples.

The results of the tests show very little spread in the standard deviation of the readings. This can be interpreted as evidence of the consistency of the samples due to the careful preparation and testing of the samples.

Although the material used in these tests, paper, is not a material used in motor insulation it is nevertheless fragile enough to simulate the worst extremes of motor inter-turn insulation. In the tests done it may be concluded that weak points in inter-turn insulation have been simulated effectively. The tests have shown that the breakdown level for inter-turn insulation is more or less constant regardless of the turn considered, provided the earth capacity of the coil is minimised. It also appears that the discharge test causes little or no damage to the insulation provided a reasonable number of discharges are imposed on it. The test can thus be safely used to test inter-turn insulation without causing the coil breakdown characteristics to change.

down voltage does not appear to lower the breakdown voltage of the samples.

The results of the tests show very little spread in the standard deviation of the readings. This can be interpreted as evidence of the consistency of the samples due to the careful preparation and testing of the samples.

Although the material used in these tests, paper, is not a material used in motor insulation it is nevertheless fragile enough to simulate the worst extremes of motor inter-turn insulation. In the tests done it may be concluded that weak points in inter-turn insulation have been simulated effectively. The tests have shown that the breakdown level for inter-turn insulation is more or less constant regardless of the turn considered, provided the earth capacity of the coil is minimised. It also appears that the discharge test causes little or no damage to the insulation provided a reasonable number of discharges are imposed on it. The test can thus be safely used to test inter-turn insulation without causing the coil breakdown characteristics to change.

5.6 VARIOUS EFFECTS OBSERVED CONCERNING THE CAPACITIVE DISCHARGE TEST

5.6.1 The discharge between turns

To observe the effects of the inter-turn discharge on the coil insulation a number of deliberately overstressed coils were dissected and examined. The typical results of an inter-turn flashover are shown in photograph 3, which is of a coil with the main ground insulation removed. Extensive blackening of the conductor covering has occurred. This is not due to carbonising of the insulation, but is merely a loose covering of fine particles as is found after an arc has occurred between metallic electrodes. Damage to the conductor insulation has occurred only at the small regions where the arc has left or rejoined the metallic conductors. It would appear that the arc has travelled between the ground insulation and the conductor wrapping, jumping across the thickness of several conductors. This appeared to be the normal procedure and no case was detected where breakdown occurred directly in the space of linear field configuration between the conductors. All breakdowns tended to enter and leave from the region of high stress at the radius at the edge of the conductor. A high proportion of breakdowns occurred in the overhangs of the coil. Not enough coils were examined to constitute a reasonable study. It would be of interest if such a study were to be done as it is certain that two facts would be revealed.

These are:-

1. The overhang inter-turn insulation is weaker than the main insulation where the coil passes through the stator. This is possibly because the stator region is compressed and heat cured causing voids between the edges of conductors to be minimised and removing the line of weakness between ground insulation and conductors.
2. The inter-turn insulation is damaged by the coil pulling operation.

Having the overhang region slightly weaker than the slot region is actually desirable when one considers that a breakdown within the slot could cause extensive damage to the

motor iron. Because of this, accurate control of overhang strength would be an aid to efficient motor design.

As mentioned before, it appears that the inter-turn discharge usually occurs between a number of conductors. All coils displayed this characteristic. When tests were first run an artificial coil of solenoid form was used for finding the most effective circuit arrangement. The solenoid consisted of 30 turns of 20 swg enamelled wire wound on a 6cm diameter former. It had an inductance of 54 microHenries, a value similar to that of normal motor coils. It was found that if two of Kritzinger's capacitors were used in series, a breakdown occurred at 60 KV, whereas one capacitor produced a breakdown at 40 KV. This led to an investigation of actual coil voltages and the elimination of stray inductance in the circuit. It was noticed during these tests that discharges always took place between conductors separated by a number of turns. The path of the discharge could be followed from marks left on the wire at the entry and exit points of the discharge. These never existed on adjacent wires, but varied from two wires apart to the full length of the coil.

In both this artificial arrangement and in the real coil a situation may exist where where relatively strong insulation (with occasional weak points) exists around the conductors with essentially an air path along the surface of the conductors. Investigating this situation quantitatively yields an explanation.

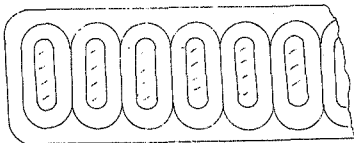


Figure 5.19 Coil section

Consider in Figure 5.19, a coil having n turns and which breaks down over x turns when a voltage V is applied to the coil. Presume that the conductor insulation has a breakdown value of a volts and the weakness alongside the conductors, a breakdown strength of b volts. No account is taken of field distortions decreasing breakdown levels.

The voltage per turn is $V_t = \frac{V}{n}$

Therefore the voltage across the turn is

$$V_x = V_t \cdot x = V \frac{x}{n} \text{ volts}$$

When breakdown occurs this is equal to the breakdown voltage $a+(x-1)b+a$

$$\text{i.e. } V_x = V \frac{x}{n} = 2a+(x-1)b$$

$$\text{therefore } V = \frac{2na}{x} + nb - \frac{nb}{x}$$

Finding maxima and minima by differentiating and equating to 0

$$\frac{dV}{dx} = -\frac{2na}{x^2} + \frac{nb}{x} = 0$$

$$\text{i.e. when } 2a = b$$

This means that the coil has maximum strength when the voltage between turns is equally likely to break down the two layers of insulation separating conductors or to jump what is essentially an air gap the width a factor. It can be seen from this that if $2a > b$ then discharge tends to take place across a number of conductors except if by chance there are two adjacent weaknesses in the conductor insulation. In the coils studied it would appear that $2a$ is always greater than b . It would appear that there is thus little point in providing strong inter-turn insulation as a precaution against breakdown between turns due to surfaces, unless measures are taken to eliminate lines of weakness between conductors and ground insulation.

In photograph 4 are shown some typical cross-sections

of coils. These illustrate these weak points and show how they occur. This is due to the wrapping of the ground insulation which is done in the form of a tape which is wrapped around the bunch of conductors. This is done specifically to stop breakdown from occurring between ground and the conductors due to the full potential of the motor supply voltage. This it does effectively because a discharge must pierce the tape, or go round it, via a long discharge path. Care is taken to wrap the tape tightly to avoid voids which may cause partial discharges. However there is no evidence that action is taken to avoid a discontinuity between ground insulation and conductor insulation. It is along this discontinuity, especially in the overhang, that inter-turn discharges occur. To prevent this it is proposed that far greater care be taken to fill this discontinuity.

Experimental work is described in Chapter 7 which examines this breakdown effect in practical detail.

5.6.2 Noise on the discharge waveform

Jones observed in his study that a large amount of noise occurred on his oscilloscope trace. His measurements were taken on the current waveform which exhibits excessive noise of this nature, as is seen in photograph 5. It is seen that this noise, which is of a high frequency nature, occurs at the current maxima. It is interesting to compare this with the voltage waveform as in photograph 1. This also exhibits noise although not as greatly as the current waveform. This noise is also coincident with the peaks of the waveform. Although it appears that this noise is provided by the same source, this is not possible as current and voltage are out of phase by 90° .

If it is presumed that the noise is due to current or voltage reversals in the circuit, the voltage noise is caused by the current reaching zero when the spark gap has a tendency to become non-conductive again because there are insufficient charged ions flowing across the gap to maintain the ionised path from a heated cathode region emitting electrons. The current can only be re-established in the opposite direction when the voltage across the inductance

collapses sufficiently to cause the voltage across the gap to re-establish the arc. This occurs at a relatively low voltage due to the large amount of ions still present in the gap, which swiftly causes a cathode to be established on the other side of the gap. As evidence of this, a picture of the voltage waveform in the region of the discharge extinction is presented (photograph 6). Here is seen the collapse of the voltage which must exceed approximately 350 volts before the arc may be re-established. When this is no longer possible the arc extinguishes.

It is presumed that the equivalent type of phenomena occurs with the current waveform when the voltage across the gap reverses. When this happens there is insufficient voltage to maintain ionisation and the current collapses due to the inability of the gap to conduct without a voltage across it. This leads to a violent noise waveform as ionisation is re-established.

6 RADIO FREQUENCY COIL TESTING

To achieve a reasonable test potential between the turns of a coil without drawing excessive current implies having a high impedance coil. An uninserted motor coil has too low an inductance to achieve this at power frequencies and a test waveform having high frequency components is required. For example, a 100 microhenry coil would have an impedance of 0.03 ohms at 50 Hz, whereas at 1 MHz the same coil would have an impedance of 600ohms. To achieve a total coil voltage of 1 KV would therefore respectively require 33 KA or 1.7 A of current.

The simplest test waveform to achieve this is a continuous sine wave of the correct frequency. This may conveniently be produced by an electronic circuit. Little information is available concerning this method. An extensive search of the literature failed to reveal references to any continuous radio frequency tests of solid insulating materials. A local motor winding firm, L.H.Marthinusen Ltd. has a piece of equipment of uncertain vintage which is designed to perform such a test on induction motor coils. The values of voltage induced and frequencies needed by this tester could not be ascertained from the user. The circuit appeared to be a single valve oscillator which coupled inductively with the test coil. As it had to be tuned for a minimum grid voltage at resonance, it is presumed that the circuit is very similar to that of the familiar grid dip oscillator used by radio workers to ascertain the resonant frequency of circuits (see figure 6.1).

This test was applied only in special cases and even then appeared to be used more to discover inter-turn short circuits than to scientifically stress the insulating material. The test was conducted by placing the test coil within the magnetic influence of the test circuit and then tuning the circuit to the self-resonant frequency of the coil by observing the dip on an ammeter connected to the grid. Proper class C oscillations caused the minimum current to flow in the grid circuit. The supply voltage was raised until the desired potentials were achieved. If the coil

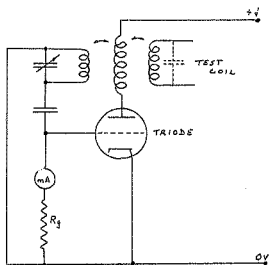


Fig. 6.1 Grid dip oscillator

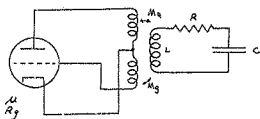


Fig. 6.2 Meissner oscillator

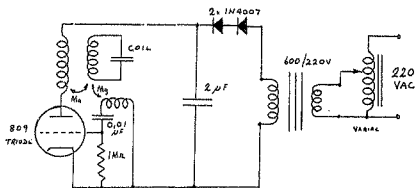


Fig. 6.3 Practical Meissner oscillator

flashed over internally then the resonant frequency and Q of the coil changed causing the grid dip meter to rise as the class C condition was lost.

A test method such as this one has a number of disadvantages. There is a lack of preciseness in the induced voltage levels which make the test levels difficult to determine, leading to the possibility of overstressing the insulation. If one induces very low voltage levels then this may not occur, but it negates the usefulness of the test in not stressing the insulation close to limits which would reveal potentially weak coils. As the voltage level is dependent on the coupling between oscillator and the test coils it can obviously vary over a large range depending on the proximity of the coils and their orientation to each other as well as to the number of turns on the test coil.

Another disadvantage is that the circuit must be re-trimmed for each coil so as to obtain the optimum grid dip. If the circuit were self-tuning, and determined its frequency purely from the self-resonant state of the test coil then testing would be speeded up. All that would be required would be to present the test coil to the circuit for oscillations to commence.

A circuit capable of doing this is one based on circuit known as a Meissner Oscillator [40]. The theoretical circuit is that shown in Figure 6.2. The condition for maintained oscillations is

$$\frac{M_a}{R_a} (\mu M_g - M_a) > \frac{R}{\omega^2}$$

where M_a is the mutual inductance between the anode coil and the test coil.

M_g is the mutual inductance between the grid coil and the test coil.

μ is the voltage amplification factor of the valve.

R_a is the plate resistance of the valve

R is the equivalent series resistance of the test coil (and other coupled components)

ω is the angular velocity of the oscillations

$W = 2\pi f$ where f is the frequency.

Obviously a prime requisite for oscillation is that

$$\frac{M_a}{M_g} < \nu$$

Thus a large ν is an advantage; also a large M_g . It would appear that a small M_a would be an advantage, however this conflicts with the other appearance of M_a in the equation and M_a is best maintained in terms of M_g . A low value of plate resistance R_a is also indicated. Most important, a high frequency and low effective series resistance in the test coil may be indicated. This is important under breakdown conditions as the effective parallel resistance decreases suddenly i.e. effective series resistance increases. Oscillations will then cease when a breakdown occurs.

A practical circuit employing this principle is shown in figure 0.3. It has the advantage of automatically resonating the coil as well as certain safety features. The coil could be placed in the live circuit and oscillations would commence. If the operator was in metallic contact with the coil conductor then sufficient effective series resistance was introduced to damp the oscillations. The circuit had the disadvantage that oscillations were not always produced, probably due to some or other infringement of the maintenance conditions above. Under these circumstances a certain amount of juggling of the test coil was required to obtain the required M_g . The test also suffered from the disadvantage of not having a standard test frequency, independent of the coil being tested. As the breakdown potentials of solid insulations are very frequency-dependent, this could be a grave disadvantage where consistent testing is required. For this reason the test circuit is only recommended for non-rigorous, fast checking of coils by unskilled personnel where a certain safety element is required.

For rigorous testing a different approach is required. Although the principle of induced high frequency voltages is still required, to obtain the correct frequency stability a circuit must be designed which will oscillate independent-

ly of the test coil. A powerful oscillation is required which will produce a strong high frequency magnetic field. After a number of experiments with several different types of oscillator circuits, it was decided to employ a series-fed Hartley oscillator. This is a simple oscillator to operate due to the strong out of phase coupling between anode and grid. It tends to employ virtually all of the voltage swing available from the supply and is not easily affected by outside influences. The theoretical circuit is shown in figure 6.4. A description of the mode of operation may be found in most electronics textbooks [41].

A practical Hartley oscillator is shown in Figure 6.5. The test coil is placed in the proximity of the oscillator coil and a suitable voltage induced into it. The oscillation frequency is controlled by changing the coil (coarse control) or varying the variable capacitor (fine control). The induced voltage in the test coil may be varied by moving the coils or more conveniently by adjusting the supply voltage via a Variac. The circuit shown is sufficient to excite the normal type of induction motor coil to 2 KV, which for reasons outlined in Chapter 7 later, is more than sufficient to adequately stress the coil insulation.

In all the circuits so far discussed the main difficulties likely to be encountered are those connected with the measurement of voltage. What is required is a device which presents little or no load and which is simple to operate, preferably of a go/no go variety. An oscilloscope with a high voltage attenuating probe fulfills this condition partly and acts as a means of checking any other device. As in the previous chapter, it was thought that using a spark gap would provide a ready means of achieving this detection. Unfortunately at normal atmospheric pressure the distances involved tended to be rather small. This meant that any change in the effective gap dimensions had a very marked effect on breakdown voltage. This included temperature effects, dirt on the electrodes or electrode erosion. After several unsuccessful attempts to produce a reliable spark gap the idea was dropped and a different approach adopted.

A glass tube was designed with an electrode at either

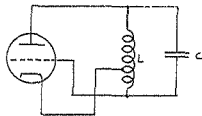


Fig. 6.4 Hartley oscillator

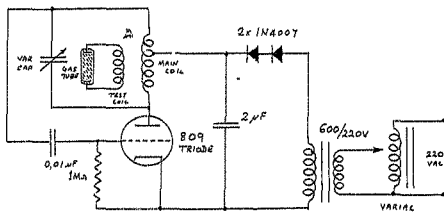
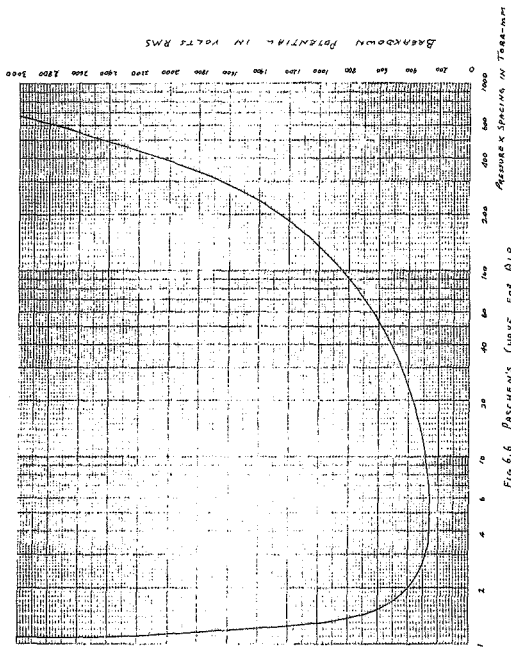


Fig. 6.5 Hartley oscillator for coil testing

end connected to wires which passed through the glass. The tube was evacuated to a low pressure sufficient to ensure that breakdown occurred at the correct voltage. This could be varied by changing the dimensions or internal pressure. These figures could be roughly determined from Paschen's Curve (figure 6.6) taking into account that the curve applies to uniform fields. Such a tube was constructed as shown in figure 6.7. The end electrodes were made of pure nickel sheet derived from a vacuum tube anode and the lead out wires were platinum to ensure a reasonable gas seal. The gas in the tube was air at a pressure of 1mm of mercury.

When the tube was tested it was found to work well, with certain desirable properties. Instead of breakdown at a set voltage, there was a far more gradual effect. At a certain lower voltage, 1,6 KV in this case, a pink glow would be observed starting at the electrodes. It was found that the pink glow spread with increasing voltage until at 2,2 KV it met in the middle whereupon a brighter glow was observed from the gas as though more current was being passed, breakdown being complete. This was a typical corona glow, as is often experienced at high frequencies.

Corona tends to occur readily at high frequencies due to the effect of ions moving backwards and forward under the influence of the alternating electric field. In a normal D.C. corona such ions may cause one or two further ionisations before being swept away or collected by the electrode. In the case of a high frequency A.C. field the field would reverse before this could happen and an ion can readily move back to its original position. If the energy it acquires is sufficient to cause further ionisation then a belt of ionisation builds up readily around the conductor as the only means of ion loss is then by drift or recombination. As the electrons are more mobile and therefore still readily lost, recombination is not usually significant. Obviously ionisation will only build up where the field is sufficiently intense to cause the production of further ion pairs by collision. This is the case close to the electrodes. In the middle of the tube, although there are ions oscillating in the field, they do not acquire enough energy to



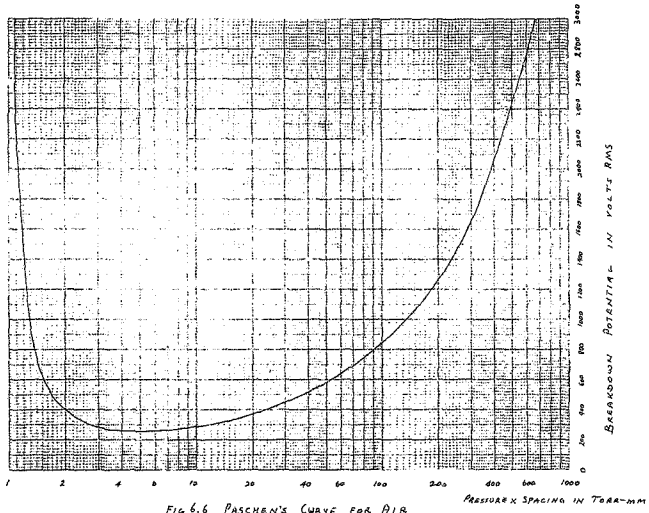


FIG 6.6 PASCHEN'S CURVE FOR AIR

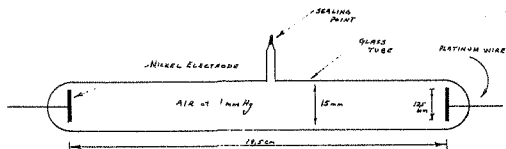


Fig. 6.7 Discharge tube

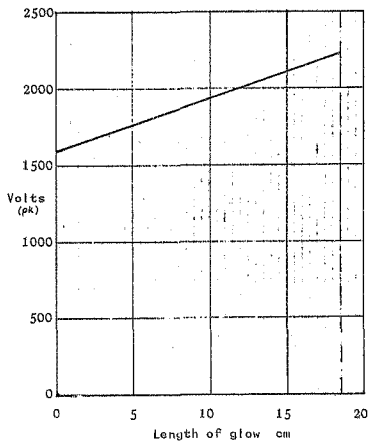


Fig. 6.8 Discharge tube behaviour at 1.0 MHz

cause ionisation until the voltage is raised sufficiently.

The discharge tube connected across the test coil thus acts as a voltmeter with the length of the discharge giving a measure of the voltage according to figure 6.8. This allows a range of measurement on each tube and lessens the number of tubes required for a large range of test voltages. There is also much to recommend deliberately designing a tube with a very non-linear field arrangement so as to utilise this effect and increase the range of measurement. Unfortunately this was not possible due to lack of time and facilities for glass blowing, this type of work having to be done by another department of the University.

The tube may be used to detect breakdown as in the previous chapter. If an internal breakdown occurs then insufficient voltage will be available at the coil ends to cause the tube to glow and the coil is rejected. Such a means of detection lends itself to rapid testing of coils by relatively unskilled personnel.

Provided that an effort is made to eliminate direct contact with the oscillator circuit, this method is a safe one to operate. Contact with high voltage radio frequency voltages leads to a flow of current through the outer layers of the body only, due to skin effect. Thus the current is confined to the outer layer of the subject's skin, which has a high resistance. It does not pass through vital organs. At the point of contact a rather painful surface burn is experienced. To test this hypothesis tests were done on a typical coil test arrangement of the Hartley Oscillator type. It was found that with the radio frequency energies required to test coils, voltages of up to 1 KV peak could be sustained without more than a small burn on the skin. Although small, it was nevertheless painful and would cause any operator to immediately drop a live coil.

Despite all the advantages of coil testing using high frequency voltages there still remains one major stumbling block and that is that high frequencies interact with the insulation tested and transfer energy to it during the test. This transfer of energy may be in the form of electrical hysteresis or partial discharges. Either way sound insu-

lation may be damaged causing failure immediately or at a much later date. This means that high frequency testing must be done very carefully to avoid any sort of damage to the insulation. Contrast this with the performance of solid insulations under impulse conditions where only the intrinsic strength of the insulation is of importance. With high frequency voltages, the breakdown is because of thermal or discharge phenomena. For this reason the test method becomes critical as it is affected by the ability of the insulation to eliminate heat. This will be dealt with practically in the following chapter. A theoretical prediction of R.F. heating is beyond the scope of this study.

It would appear from these reservations that a radio frequency means of testing is not to be advised where the tests are applied to critical components. It may be conveniently applied to coils in a routine testing role where the R.F. voltages used are insufficient to damage coil insulation. It should never be applied where the effects of such voltages on the particular insulation are unknown.

7 Practical breakdown tests performed on a number of insulating materials.

7.1 Introduction

A knowledge of the performance of real materials is required to effectively test coils using the five basic methods. Comparative tests have been done on a number of samples using the standard impulse (1,2/50), a standard capacitive discharge waveform and a continuous R.F. sine wave. Samples used included material in sheet form as well as portions of real coils.

7.2 Tests on real coil samples.

Due to their high cost only a limited number of induction motor coils were available for test, these being supplied by a local motor repair firm. It was decided to test two such coils, one insulated between turns with epoxy resin and glass fibre, the other with alkyl enamel and glass fibre.

To obtain the maximum use out of such a limited number of coils it was decided to sectionalise the coils, producing short lengths of conductors still bound together by the ground insulation. These were then tested by applying the various tests between the conductor lengths, care being taken to ensure that the inter-turn insulation remained intact and undamaged by the sample preparation.

Care was taken to separate overhang and slot portions of the coils as these receive differing amounts of heat curing in the coil preparation and can be expected to have different properties. This was found to be so in practice.

Each sample (as detailed in Appendix E) was approximately 25 cm long. 2,5 cm of ground insulation was trimmed from each end to facilitate the connection of test voltages to the conductors. To avoid flashovers at the ends of the sample, the conductors in this region were gently fanned out, one at a time as tested and insulated with a blob of insulating grease (Penetrol). Such a prepared sample is shown in figure 7.1. Light insulating oils (transformer oil) may not be used for this purpose as penetration of this between the conductors will influence the results obtained. Although the use

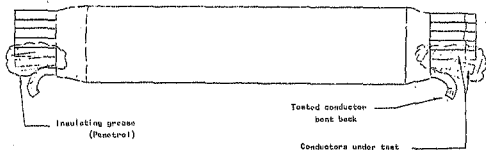


FIGURE 7.1 COIL SAMPLE

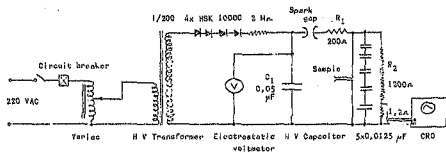


FIGURE 7.2 STANDARD IMPULSE GENERATOR

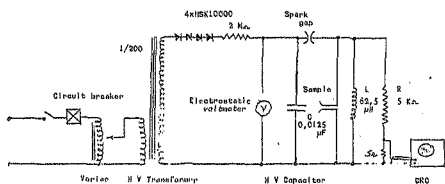


FIGURE 7.3 OSCILLATORY IMPULSE TEST

of this grease makes the sample preparation messy and tedious it is necessary if consistent meaningful results are to be obtained.

The dissected coils provided sufficient samples to allow for a standard 1,2/50 impulse test, an oscillatory impulse test, and a high frequency test at two different frequencies. One piece of overhang was available for each of these tests, along with either one or two portions of slot section. In this way it was possible to compare these differing regions of the coils.

The standard impulse test was performed on the samples using the impulse generator shown in figure 7.2. As the sample capacity was a variable quantity, it was decided to swamp it out with an external capacitor of a suitably higher value i.e. 0,0025 microFarad. The resistances were constructed out of non-inductive zig-zag type resistance tape to the values shown. The tail resistor R_2 was terminated in a small resistor which allowed the impulse voltage to be measured directly on an oscilloscope as well as permitting the wave-shape and times to be adjusted to the correct values. The main capacitor, C_1 , was one of those constructed and used by Kritzing for his work [38]. The sphere gaps, permanently attached to the capacitor, came from the same source.

The tests were done by setting the voltage on the capacitor to the wanted value and then closing the spark gap until it sparked over discharging the generator. This was done with an arrangement of linen tapes which rotated the movable sphere, screwing it in or out as needed. The initial tests were done starting at a low value, 5KV, but were later started at 14KV as breakdowns were found to be occurring at above this value. The procedure used was to give two discharges, approximately ten seconds apart, then raise the voltage by one kilovolt and repeat the two discharges after waiting at least a minute from the previous discharges. This was done until the sample finally failed, care being taken to see that this was not just an external discharge through the insulating grease at the sample ends.

The insulation thickness was obtained by measuring, with a micrometer, the thickness of the copper and insulation com-

binations as the sample was stripped down at the end of the test. This entailed many measurements and was tedious. A later method adopted was to strip the conductors out, measure them with and without insulation and average the difference to give an average figure for insulation thickness in that sample.

The oscillatory impulse test was performed on the samples according to the recommendations of Chapter 5. The circuit used is shown in figure 7.3. The value of the tail resistor shown gave waveforms of the correct decay time. The generating coil employed was a spare motor coil with a high strength between turns. It was found that the coil and capacitor used gave a test frequency within the allowable tolerance outlined in Chapter 5. The peak potential of the impulse was virtually that of the stored value on the capacitor. The test procedure was similar to that of the previous test. The sample was discharged twice at each value before waiting a minute and then discharging at one KV higher. The insulation thickness was measured as before.

The samples were radio-frequency tested with the apparatus shown in figure 7.4. A variable H.V. D.C. supply fed a series Hartely oscillator which supplied an R.F. voltage to the sample. The entire arrangement was housed in a Faraday cage made of copper sheet to prevent a leakage of radio interference. Considerable experimentation was necessary to obtain the correct combination of coil, capacitor and coil tapping point for efficient oscillations to occur. Further adjustments were needed to obtain the correct frequencies used namely 1 MHz and 2,5 MHz. Care was also required to avoid 'squeeging' (unstable bursts of oscillation) due to too high a grid capacitor resistor combination. It was also found that an amount of corona discharging took place from exposed small radii surfaces. These had to be covered over with crumpled aluminium foil to raise their effective diameters. The triode used required a supply of cooling air which was provided by a high duty fan.

Initial tests indicated that the test circuit provided a test waveform which had a peak value of almost the same level as the voltage provided by the D.C. supply. This was

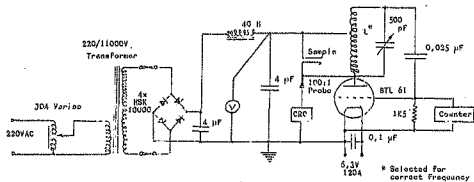


FIGURE 7.5 RADIO FREQUENCY TEST SET (HIGH VOLTAGES)

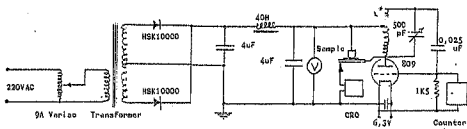


FIGURE 7.5 RADIO FREQUENCY TEST SET (LOW VOLTAGES)

determined by examining the test waveform using an oscilloscope with a high voltage probe, used up to 1000 volts, the limit of safe operation for the probe. A consistent difference of 50 volts between peak value and supply volts was indicated. For values of voltage over 1KV this was assumed still to hold and the peak of the test waveform was assumed equal to the supply voltage less this value of 50 volts.

Care had to be taken to avoid overheating the sample before breakdown occurred. The method adopted under these conditions was to raise the test voltage at a specified constant rate until breakdown took place. The rate of increase is approximately that to give the average breakdown value in ten seconds. Breakdown is indicated by a sudden drop in supply voltage as well as noise from the sample. It was found that little separation of the ends of the conductors was required as the breakdown of the solid insulation matched that of air. The thickness of the insulation was measured as before.

The condensed results of the tests on the coil samples are shown in table 7.1. These are discussed later. The original readings are presented in Appendix E.

7.3 Tests using sheet samples of insulating materials

It was decided to test two modern materials, often used for inter-turn insulation in special applications such as on hand taped overhangs. These were Kapton, a polyimide film and Nomex M, a crushed mica reinforced felted polyamide fibre paper. Both materials are available in the form of thin sheets and are typical of high performance modern insulating materials.

The impulse tests were applied as before, using the same equipment. The sample, in sheet form, was placed between two brass electrodes. The bottom electrode was a flat plate. The top electrode was a cylinder of 25 mm diameter and 25 mm long with its edges rounded off to a radius of approximately 2 mm. This rested under its own weight on the sample.

The radio frequency test was performed using a lower voltage version of the series-fed Hartely oscillator used before. As the currents and voltages involved were lower, this could use a smaller coil and power supply as well as a low power naturally cooled triode. The circuit is shown in figure 7.5. In this case a reasonable number of samples

were available and a much larger number of frequencies were used. This gave the results in the form of a curve (figure 7.6). The rest of the results are presented in Table 7.2. The original readings are available in Appendix D.

TABLE 7.1

Breakdown results from tests on dissected motor coils.

COIL 1 - 6,6 KV EPOXY DOUBLE GLASS

7 turns, coil cut to 12 pieces.

Coil breakdown = 35 KV

REGION	IMPULSE TEST	OSC. IMPULSE TEST	R.F. TEST 1MH _z	R.F. TEST 2,5 MH _z
CORE	378 KV/cm	340 KV/cm	49,0 KV(pk)/cm	44,7 KV(pk)/cm
OVER-HANG	239 KV/cm	256 KV/cm	28,7 KV(pk)/cm	31,3 KV(pk)/cm

COIL 2 - 6,6 KV ALKYD DOUBLE GLASS

9 turns, coil cut to 10 pieces.

Coil breakdown = 31 KV

REGION	IMPULSE TEST	OSC. IMPULSE TEST	R.F. TEST 1MH _z	R.F. TEST 2,5 MH _z
CORE	643 KV/cm	588 KV/cm	76,9 KV(pk)/cm	75,1 KV(pk)/cm
OVER-HANG	505 KV/cm	413 KV/cm	58,6 KV(pk)/cm	75,0 KV(pk)/cm

TEMPERATURE = 23°C - 27°C

TABLE 7.2

Breakdown of discrete insulation samples.

'KAPTON' polyimide film.

Average thickness = 0,03mm.

IMPULSE TEST	OSC. IMPULSE TEST	R.F. TEST 1MH _z	R.F. TEST 2,5 MH _z
2470 KV/cm	2300 KV/cm	180 KV(pk)/cm	165 KV(pk)/cm

'NOMEX M' mica loaded

felted polyamide fibre

Average thickness = 0,14mm

IMPULSE TEST	OSC. IMPULSE TEST	R.F. TEST 1MH _z	R.F. TEST 2,5 MH _z
650 KV/cm	596 KV/cm	122 KV(pk)/cm	108 KV(pk)/cm

TEMPERATURE = 20°C - 25°C.

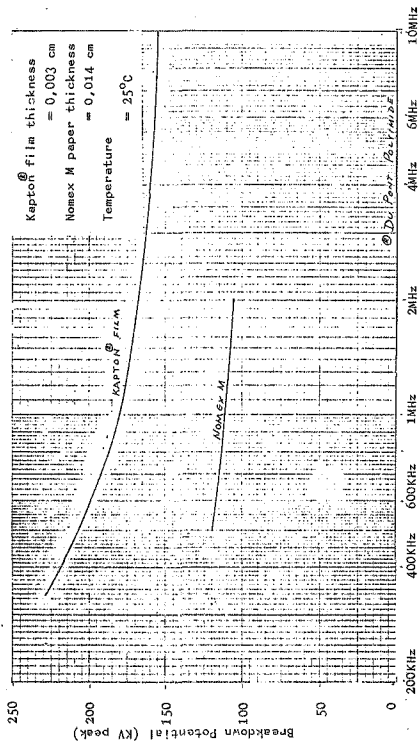


FIGURE 7.6 R.F. BREAKDOWN TESTS ON KAPTON AND NOMEX M

7.4 Analysis of the test results

A number of trends are obvious from the results of the breakdown tests.

7.4.1 Impulse tests

It can be seen that the core sections of the coil have better breakdown values than the overhang sections. This is due to the better curing and compaction that this region receives when the coil is manufactured. There is also more chance of damage to the overhang region during coil forming. It can be seen that little difference in effect exists between the two impulse tests though it would appear that the oscillatory impulse test is harsher. Breakdown values with it are about 10 per cent lower than with a standard impulse test.

It is of interest to notice that both coils would only stand about 30 to 35 KV when subjected as complete coils to the oscillatory impulse test. When individual sections of coil are subjected to the impulse tests they appear capable of withstanding about 20 KV between individual adjacent conductors. If it is presumed that the test voltage per turn is almost the same irrespective of turn position then it would appear to be an anomaly that the entire coil is weaker than any of its components. There are perhaps two explanations of this phenomena.

Firstly account must be taken of the statistical probability that a weak point exists somewhere in the coil which will cause a breakdown to take place at a much lower voltage. Obviously just one such weak point is sufficient to fail the entire coil. The probability of this weak point having a certain breakdown value depends on two factors, normal statistical variation of breakdown values and the chance of an unusual weak point in the insulation. The latter would be the case with an occluded metal particle or void or some such similar fault, and is difficult to predict reliably.

To predict the normal statistical variations of coil section breakdowns the results of all the impulse tests on coil segments were lumped to obtain a single histogram. This could be done as the samples were all approximately the same length and it was felt that as many readings as possible were needed to obtain a reliable curve to predict the statistical proper-

ties of coil segment breakdowns. The individual results of the breakdown tests were normalised by dividing them by the average for that test, taking into account that the overhang and core sections were different. For the purposes of drawing a histogram an interval of 0,05 of the normalised value was chosen. The histogram is shown in figure 7.7. To predict the behaviour of coil segments it is necessary to know mathematically how the histogram varies about the average value. For this purpose the root mean square of this variation about the mean was computed as in the Appendix E. This allowed a normalised Gaussian probability curve, with the same interval (0,05) to be plotted over the histogram. From this can be seen that there is a fair amount of correspondance between the two and it is assumed that the breakdown of coil segments follows this distribution.

Assuming that the samples obey this distribution, a statistical prediction can be made for certain failure rates (see Appendix E). For coil 2 the one per cent failure voltage is 54,4 KV with a 50% failure at 86,8 KV. As these are much higher than those in practice, a different explanation of breakdowns is forthcoming.

A far more successful approach is that based on the field situation which exists within the coil and on the voltage distribution between coil conductors where flaws exist in the insulation. This has already been partially discussed in Chapter 5, where it was observed that breakdowns tended to occur between conductors which were not adjacent.

The voltage distribution between conductors and its influence on breakdowns in the region down the sides of the conductors is complex depending on conductor shapes and insulating material distributions. This becomes even more complex when voids in the insulation are considered especially as such voids are unpredictable in extent. The situation down the side of the conductors may be recognised as a hazardous one, it being a region of mechanical discontinuity which is at right angles to a voltage gradient. Such situations are avoided in high voltage practice as experience has shown them to be dangerous.

This dangerous situation may be analysed by making some

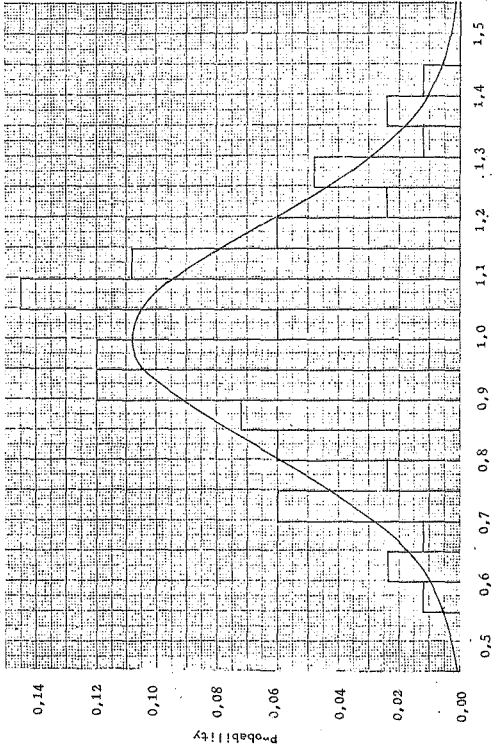


Figure 7.7 Normalised Histogram of breakdowns

assumptions concerning the nature of the coil edge region.

1. An air discontinuity exists between the turns insulation and the ground insulation and extends along this entire region.
2. The solid insulation has the same permittivity and dielectric strength over the whole region.
3. The turn insulation has the same strength as that ascertained in the tests, i.e. two separate layers of conductor covering have a combined strength equal to that of an adjacent double layer.
4. The field distribution is that which would occur in solid insulation. The discontinuities are assumed to be insignificant in size and unlikely to distort the field appreciably. Likewise it is assumed that stress concentration does not occur due to the differences of permittivity that occur between insulation and voids.

A coil of cross-section similar to that of coil 2 was considered as an example. Only four turns i.e. five conductors were considered. A potential plot was obtained in two dimensions using a conductive paper model. This is shown in figure 7.8. Any discontinuities between turn insulation and ground insulation would occur along the dashed line which indicates the join between these insulations. The conductors were raised to progressively higher voltages as shown.

From this analogue model may be deduced a number of features:-

1. High stresses occur in the regions marked A. Breakdowns are likely to be initiated in voids in this region.
2. Low stresses are present at points marked B. Breakdowns are unlikely to start at these points. It may proceed through these regions if the stress pattern is distorted by breakdowns in region A.

As the conductors are subjected to pressure when curing occurs, it may be surmised that a certain amount of material fills the region C where the conductor coverings join. The actual join between turn insulation and ground insulation is thus likely to follow the dotted lines in this region and

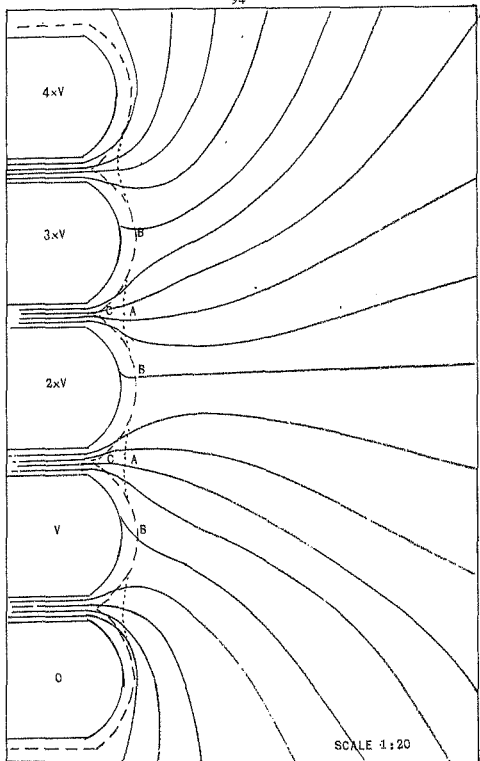


Figure 7.8 Field plot

avoids the cleft at C, which could give trouble. Measuring along these new joins gives a stress of three potential lines in 0,75 mm for the highest stressed regions, A, and about one in 1,0 mm for the low stressed region. This indicates a maximum stress of approximately

$$\frac{3}{5} V \text{ over } 0,75 \text{ mm}$$

and a minimum stress of

$$\frac{1}{5} V \text{ over } 1 \text{ mm}$$

Coil 2 broke down at 31 KV for 9 turns, giving an inter-turn voltage of 3,44 KV = V

Thus the maximum stress is 2,1 KV over 0,75 mm

Examining Paschen's curve for air (Figure 6.6) yields a breakdown voltage of 2,2 KV when pressure = 625 mmHg and $d = 0,75$ mm

It would thus appear that local breakdown in the regions of high stress would lead to a flashover between conductors due to failure down the insulation joint. Eventually a high enough voltage would be imposed across two of the conductor insulation layers to cause them also to fail. As this is likely to occur at a value close to that of the impulse tests, it may be surmised that a number of coil turns must be spanned to allow this. In the case of coil 2 this would be at 16,1 KV corresponding to the voltage across a minimum of 5 turns.

The field plot done did not take into account the limited thickness of the ground insulation around the coil. This is, however, at least ten times the turn insulation thickness and only has effect at the edge of the field plot where the stress is very low. The field at the stress points is virtually unaffected.

Similarly with the coil placed in position in the motor core the field plot would appear different. It would not, however, greatly affect the separation of the potential lines. Even though they would appear in different positions they would still tend to have the same separation and hence the same stress relationship.

From the field plot a solution to the inter-turn weakness problem is obvious. If the interface between the two insula-

tions could be made to occur further away from the conductors, say 1 mm away, then it would occur in a region of virtually uniform stress. As the stress in this region is half of that at A, the inter-turn breakdown could be doubled and it may even be found to be limited by the statistical probability of failure directly between turns. A practical method of achieving this is not obvious. The answer may be found in a technique of impregnation of a relatively loose fibre covering around the conductors. Such a covering (glass fibre), being loose, could easily be compressed to form the direct insulation between turns of the correct thickness, but would retain its looseness at the edges. These edges could then be made electrically strong by suitable impregnation and curing.

7.4.2 Radio Frequency tes.s.

Although a limited amount of information is available on R.F. breakdown in gaseous dielectrics [44,45,46], an extensive search for information on R.F. breakdown in solids revealed only one rather dubious reference by Peak [47]. It would appear that the two breakdown processes are completely different. In the gaseous dielectric case the breakdown is characterised by the behaviour of mobile ions. When a certain transition frequency is reached, corresponding to the transit time of the ions, then ions are allowed to build up in the inter-electrode space and breakdown occurs more readily. As positive and negative ions have different mobilities there are two such transitional frequencies, a fairly low frequency one due to positive ions and a high frequency one due to negative ions. The case with which R.F. voltages cause corona discharges is a further manifestation of this effect.

In solid insulation the ions are not mobile and do not observe these transitional effects. As can be seen from the results for Kapton and Nomex M, the R.F. breakdown voltage is very much lower than the impulse strength. This can be best explained by the ability of the R.F. voltage to release ions from the normally stable lattice of the dielectric material. This can be done in two ways, direct excitation and temperature effects. Nothing is known of the first effect. The second effect is from losses in the dielectric due to hysteresis. Raising the temperature of a dielectric causes

its breakdown value to drop appreciably. It can thus be seen that the R.F. breakdown of a sample is greatly affected by its ability to generate and dissipate heat. This depends greatly on the physical arrangement of the specimen as well as the presence of polar impurities, such as moisture.

The exact prediction of R.F. breakdown is difficult and is best done empirically. This is a further disadvantage of the R.F. method of inter-turn testing. Also the mechanism of breakdown is not a natural one and leads to a situation where breakdown is dependent on factors such as heat dissipation. More important is the fact that as the relative R.F. breakdown strengths of air and solid are similar the effect of voids is not critical in producing breakdown. For this reason a coil passing an R.F. test can never be relied on under surge conditions if it is likely to fail in the manner described previously, namely via voids in the insulation interface region.

8. CONCLUSION

It is recognised that a need for surge resisting motors exists. It is possible to protect ordinary motors using capacitors and surge arrestors as outlined in the references (3,4 and 12). This is not practiced as much as it should be, and would be even more effective if used with motors which are designed and tested to resist surges. Such motors are indicated for applications where surges are likely to be troublesome as is the case when the motor is in an exposed position, or when vacuum circuit-breakers are employed. When this is combined with the need to maintain continuous operation the need is most critical. This includes such operations as pumping, winding, ventilating and material handling at remote stations. Even within a safe system such motors should provide more protection where used for process, refrigeration or production applications and for essential services. Where a spare motor is on hand it usually takes a prohibitively long time to change over if one should fail electrically.

The decision to apply inter-turn tests to induction motors during manufacture is always, a financial one. The tests cannot be applied to each and every motor produced without raising the general price of the motors. This will place one at a disadvantage with regard to one's competitors in applications where surge resistance is not demanded. Likewise the limited production of surge tested and resistant motors must be accompanied by a campaign to inform customers of the advantages of using such motors. This supposes the possession of statistical information on motor failures, something which the manufacturers are better able to gather than anyone else.

It may also be of advantage to produce a number of different classes of surge resistant motors, the aim being to minimise costs in relation to the application intended. The most expensive and reliable motor would be one using all tested coils, with the full 20 KV per microsecond per KV of motor supply as detailed earlier. This would give a certain test voltage dependent on surge propagation velocity, size and number of turns of the particular motor coil. An intermediate class of motor may be arrived at by specifying tested coils only at the criti-

cal line end of the motor. Alternatively full rated coils may be used in this position with half rated (10 KV) coils used elsewhere, or half rated coils throughout."

The full rating referred to is based on a study of currently available information on lightning surges. Most of this information is American in origin. It is felt that a thorough study of fast lightning impulses on South African power systems would be useful in clarifying the position. Work is also indicated on vacuum circuit breaker induced surges and their effects on motor windings.

It is felt that manufacturers have little to gain by an exhaustive study of surge propagation phenomena in motor coil assemblies. As is shown, such a study is complicated and can be liable to errors out of proportion to the effort involved in computing them. A simplified model, as proposed, when combined with a practical study of the actual coil yields useful results which are able to be utilised in design. A sound basic principle is to take a course of action which limits the transmission line behaviour of the coil and which encourages the energy of the surge front to be dissipated uniformly and swiftly over the entire coil. On this basis the coil requires low capacity to ground, high inter-turn capacity, low self inductance and high mutual inductance between turns. These properties are in conflict with the use of thick insulation between turns and, as in any insulation design, there is an optimum thickness of insulation which gives the maximum potential withstand within certain physical constraints.

The radio frequency method of coil testing is subject to the limitations outlined in Chapter 6 and should only be used where conditions demand a safe, swift and non-exact method of inter-turn testing. It is felt that by applying a little thought the impulse method may be simplified and speeded up to make it just as easy to apply as the radio frequency method. Where a large number of coils are to be tested then this becomes justified.

To aid effective design of coils and to prevent failure due to surge induced breakdowns between turns, more is required to be known about the actual breakdown process. As has been demonstrated, knowledge of the breakdown strength between turns

does not imply a knowledge of the surge strength of the coil. This can be much lower than the inter-turn strength would lead one to believe, due to the stress concentration in the critical interface between turn insulation. The effects of differing insulating materials may be particularly significant. The only effective method of analysing this is by field plotting followed by a practical breakdown test to confirm one's findings.

One of the aims of any project such as this one is to provide design material and improved methods of construction and testing of motors. Although hampered by a lack of material it is hoped that the methods employed here are an aid to the production of improved induction motors for South African conditions.

APPENDIX ACharacteristics of Lightning Arresters1. American Practice

The following table was taken from:-

AIEE Lightning Arrester Subcommittee "Station-type
Lightning Arrester Performance Characteristics"

AIEE Trans, Volume 59, June 1940. pp 347-348

AIEE wave is a wave rising at the rate of 100 KV/microsecond
for every 12 KV of arrester rating until sparkover occurs.

Arrester Rating KV rms	Sparkover Voltage		I.R Discharge Voltage				
	1,5x40 wave KV	AIEE wave KV	KV				
			1500A	3000A	5KA	10KA	20KA
3	10	13	9	10	10	11	12
6	19	23	18	19	20	22	24
9	27	35	27	29	30	33	35
12	39	43	36	38	40	44	47
15	49	53	45	47	50	54	59
20	66	72	60	64	67	72	78
25	78	89	74	79	83	90	100

2. European Practice

From

IEC Publication 99/1 2nd Edition

Arrester Rating KV	Sparkover KV 10 KA rated arresters
3	13
6	22,6
10.5	38
12	43

Note This is for wave similar to AIEE wave.

3. Australian Practice

From

Australian Standard C338 - 1965 Surge Diverters

Arrestor Rated KV	1.2x50 wave KV Sparkover	Wavefront test	
		Front steepness KV/msec	Sparkover KV
3	13	25	15
6	22.6	50	26
10.5	38	87	44
12	43	100	50

This is for 10KA rated arresters.

4. South African Practice

There is no S.A.B.S. standard as yet although one is in preparation. The ESCOM specification EED 8/3 is given, which will be the same basis of an eventual S.A.B.S. specification.

Arrestor Rated KV	1.2x50 wave sparkover per unit of rated volts	Maximum permissible lead drop KV
25	3.3	15
25 to 150	2.8	25
150	2.6	35

Also given is the Impulse Coordination Specification. It is generally felt that these are slightly high.

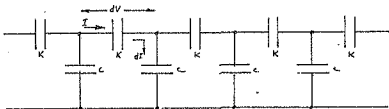
IMPULSE COORDINATION- ESCOM SPECIFICATION

Nominal system voltage KV	Arrester rated voltage KV	Arrester sparkover for impulse and switching surge, KV	Protective level at arrester KV	Required external BIL, KV	Past ESCOM external BIL, KV	Proposed ESCOM BIL KV
3.3	3.6	12	27	41	54	45
6.6	7.2	24	39	59	80	75
11	12	40	55	84	102	95
22	24	80	95	144	160	150
33	29	82	107	163	215	200
	36	101	126	191		
44	39	110	135	205	270	250
	48	135	160	243		
66	58	163	188	285	375	350
	75	204	229	347		
88	78	219	244	370	408 (485)	380 (450)
	(97)	(272)	(297)	(450)		
132	116	325	350	531	592 (700)	550 (650)
	(145)	(406)	(431)	(653)		
154	136	382	407	617	700	650
220	196	510	545	826	900	825
275	240	624	659	1000	1130	1050
330	290	754	789	1200	1300	1300
400	336	873	908	1380	1550	1425
500	420	1093	1128	1710	-	1800
725	612	1590	1625	2470	-	2550

- NOTES: 1. Data for possible future voltages of 500 and 725 KV is preliminary and is given for guidance in considering possible applications of these voltages.
2. Bracketed values are for Full insulation and 100% arresters and will not be used on new equipment unless the system is not effectively earthed.

APPENDIX B

B.1 Theoretical capacitor divider chain



K = capacity between turns per turn

C = capacity to ground per turn

$$dV = \frac{I}{j\omega K} dx \quad \dots 1$$

Therefore

$$\frac{dV}{dx} = \frac{I}{j\omega K} \quad \dots 2$$

Similarly

$$dI = jV\omega C dx \quad \dots 3$$

and

$$\frac{dI}{dx} = jV\omega C \quad \dots 4$$

Therefore

$$\begin{aligned} \frac{d^2V}{dx^2} &= \frac{1}{j\omega K} \frac{dI}{dx} \\ &= \frac{jV\omega C}{j\omega K} \\ &= V \frac{C}{K} \\ &= V \left(\sqrt{\frac{C}{K}}\right)^2 \quad \dots 5 \end{aligned}$$

Let

$$\sqrt{\frac{C}{K}} = g$$

Then

$$\frac{d^2V}{dx^2} = Vg^2 \quad \dots 6$$

This is a differential equation with general solution of the form

$$V = Ae^{gx} + Be^{-gx} \quad \dots 7$$

where A and B are constants

Using the fact that $V = 0$ at $x = 0$ and $V = U$ at $x = n$, where n is the total number of coils, and solving for A and B yields a solution

$$V = \frac{U}{2\sinh ng} (e^{xg} - e^{-xg})$$

$$= U \frac{\sinh xg}{\sinh ng} \quad \dots 8$$

If the coils are numbered from the high potential end then the potential on coil m is

$$V = U \frac{\sinh (n-m)g}{\sinh ng} \quad \dots 9$$

B.2 Theoretical turn potentials due to electrostatic field

Coil 1 has the following parameters

$$L = 94 \text{ pF}$$

$$C = 219 \text{ pF}$$

This yields

$$g = 0,86$$

allowing the approximation

$$U_1 = U \frac{e^{(n-1)g}}{e^{ng}} = U e^{-0,86} = 0,43U$$

Similarly

$$U_2 = 0,20U$$

This does not agree with the measured potential.

APPENDIX CC1 Model coil dimensions and parameters

Coil consists of ten turns of 21 SWG copper wire suspended in air above an aluminium foil earth plain as shown.

Model coil No 1

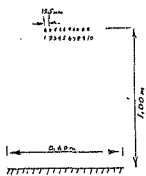


Figure C.1 Cross section of coil
(0.60m)

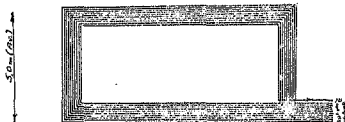


Figure C.2 Plan of coil

Coil parameters as measured on General Radio bridge

$$C_{0-1/E} = 219 \text{ pF} \quad L_{(0-1)} = .55 \mu\text{H}$$

$$C_{1-2/E} = 218 \text{ pF} \quad L_{(1-2)} = .55 \mu\text{H}$$

$$C_{0-2/E} = 270 \text{ pF} \quad L_{(0-2)} = 172 \mu\text{H}$$

$$C_{0-10/E} = 395 \text{ pF} \quad L_{(0-1)+(2-1)} = 50 \mu\text{H}$$

$$C_{0-1/1-2} = 294 \text{ pF} \quad L_{(0-5)} = 825 \mu\text{H}$$

$$C_{0-1/1-10} = 342 \text{ pF} \quad L_{(0-10)} = 2.9 \text{ mH}$$

Surge impedance of single turn = 500 ohms (calculated)

= 500 ohms (measured)

Model coil No 2

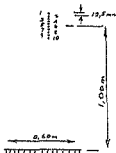


Figure C.3 Cross section - Model coil No 2

Plan as in figure C.2

Coil parameters (GR bridge)

$C_{0-1/E}$	= 221 pF	L_{0-1}	= 55 μ H
$C_{1-2/E}$	= 225 pF	L_{0-2}	= 175 μ H
$C_{0-10/E}$	= 405 pF	L_{0-5}	= 835 μ H
$C_{0-1/1-10}$	= 342 pF	L_{0-10}	= 2,84 mH
$C_{0-1/1-2}$	= 294 pF		

Surge impedance of single turn = 500 ohms (calculated)
 = 360 ohms (measured)

Model coil No 3

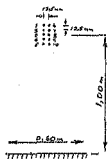


Figure C.4 Cross section - Model coil No 3

Plan as in figure C.2

Coil parameters (GR bridge)

$C_{0-1/E}$	= 220 pF	L_{0-1}	= 55 μ H
$C_{0-10/E}$	= 349 pF	L_{0-10}	= 3,25 mH

Surge impedance of single turn = 500 ohms (calculated)

Model coil No 4



Figure C.4 Cross section - Model coil No 4

Plan as in figure C.2

Coil parameters (GR bridge)

$$C_{0-1/E} = 932 \text{ pF}$$

$$L_{0-1} = 53 \mu\text{H}$$

$$C_{0-10/E} = 8360 \text{ pF}$$

$$L_{0-10} = 2,63 \text{ mH}$$

$$\text{Surge impedance of turn} = 127 \text{ ohms (calc)}$$

$$= 130 \text{ ohms (meas)}$$

C.2 Real motor coil

Manufacturer - GEC

Motor - 1272 KW (1705 HP), 6600V, 134A, 990 RPM, 50 Hz

Slots - 72, 13,5 mm x 77 mm

Conductor - copper, 9,0 mm x 4,5 mm (bare)

9,5 mm x 5,0 mm (covered)

Insulation - Class B - Polyamide enamel + double glass and epoxy resin

Coil - turns - 6 per coil

length - slot = 930 mm

overhang = 420 mm

turn = 2,70 m

coil = 16,20 m

Inductance = 260 μH (in motor)= 67 μH (in air)

Capacity (coil to stator) = 2400 pF

Four coils used were adjacent and overlapping each other

APPENDIX D

Analysis of simplified impulse generator

$$i_1 = i_2 + i_3$$

Therefore

$$C \frac{dV}{dt} + \frac{V}{R} + \frac{1}{L} \int V dt = 0$$

Differentiating this expression

$$C \frac{d^2 V}{dt^2} + \frac{1}{R} \frac{dV}{dt} + \frac{1}{L} V = 0$$

This is an equation of the form

$$D^2 + \frac{1}{CR} D + \frac{1}{LC} = 0$$

and has a solution

$$D = \frac{-1}{2CR} \pm \sqrt{\left(\frac{1}{2CR}\right)^2 - \frac{1}{LC}}$$

In the underdamped case

$$\frac{1}{LC} > \left(\frac{1}{2CR}\right)^2$$

Letting

$$a = \frac{1}{2CR} \quad \text{and} \quad b = \sqrt{\left(\frac{1}{2CR}\right)^2 - \frac{1}{LC}}$$

gives a solution of the form

$$V = e^{at} (K_1 \cos bt + K_2 \sin bt)$$

If the voltage on the capacitor is V_c at $t = 0$ then

$$K_1 = V_c$$

and if $V = 0$ at $bt = \frac{\pi}{2}$ then

$$K_2 = 0$$

Thus

$$V = V_c e^{at} \cos bt$$

In terms of the frequency of oscillation

$$b = 2\pi f$$

Therefore if $\frac{1}{LC} \gg \left(\frac{1}{2CR}\right)^2$

$$f \approx \sqrt{\frac{1}{4\pi^2 LC}}$$

APPENDIX E1. Reading of Impulse Tests

Coil 1

Diamond coil - 6,6 KV

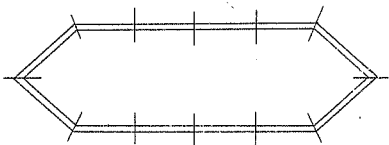
7 turns of 3,5x0,2 mm copper

Insulated with epoxy-glass between turns and epoxy-mica-glass to ground.

Inductance = 72,5 μ H

Oscillatory impulse test failure = 35 KV

Coil cut into 12 pieces as shown



1(a) Standard Impulse Test
 IEC Standard 1,2/50 impulse
 Temperature = 25°C

Region	Breakdown (KV)	Average Breakdown	Normalised Breakdown	DIFF ²	Thick-ness
over- hang	22,0	23,2 KV ≈ 239 KV/cm	0,95	0,0025	Av. = 0,97mm
	22,5		0,99	0,0001	
	24,5		1,03	0,0004	
	23,0		0,99	0,0001	
	21,0		0,91	0,0081	
	20,0		1,12	0,0144	
core	23,0	23,05 KV ≈ 378 KV/cm	0,97	0,0009	Av. = 0,61mm
	23,0		0,97	0,0009	
	21,0		0,89	0,0121	
	21,5		0,91	0,0081	
	20,0		1,10	0,0100	
	27,0		1,14	0,0196	
	14,0		0,62	0,1444	
	20,0		0,89	0,0121	
	10,0		0,84	0,0256	
	32,0		1,42	0,1764	
	31,0		1,38	0,1444	
10,0	0,84	0,0256			

1(b) Oscillatory impulse test

$$f = 180 \text{ KH}_z$$

$$T_1 = 50 \text{ sec}$$

$$\text{Temperature} = 26^\circ\text{C}$$

Region	Breakdown KV	Breakdown average	Normalised breakdown	Diff ²	Thick-ness (mm)
over-hang	29,5	26,4 KV $\cong 50 \text{KV/cm}$	1,11	0,0121	1,06
	27,5		1,04	0,0016	1,00
	32,5		1,23	0,0529	1,04
	28,0		1,05	0,0025	0,98
	22,5		0,85	0,0225	1,00
18,5	0,70	0,0900	1,10	av= 1,03mm	
core	25,0	23,1KV $\cong 340 \text{KV/cm}$	1,08	0,0064	0,74
	29,0		1,25	0,0625	0,73
	10,0		0,82	0,0324	0,65
	24,0		1,03	0,0009	0,66
	21,0		0,90	0,0100	0,59
	18,0		0,77	0,0529	0,68
	21,0		0,90	0,0100	0,67
	21,0		0,90	0,0100	0,68
	26,0		1,12	0,0144	0,74
	20,0		0,86	0,0176	0,70
	32,0		1,38	0,144	0,63
21,5	0,90	0,0064	0,68	av= 0,68mm	

1(c) R.F. test

Frequency = 1,0 MHz

Temperature = 22°C

Region	Breakdown (peak KV)	Average breakdown	Thickness mm	
over- hang	3,0	2,75KV 28,7KV/cm	1,07	av= 0,97mm
	1,9		0,89	
	2,2		0,89	
	3,2		0,89	
	3,3		0,77	
	3,0		1,26	
core	2,3	2,89KV 49,0KV/cm		av= 0,59mm
	3,5			
	2,9			
	2,2			
	3,0			
	2,4			
	2,9			
	3,4			
	2,8			
	3,0			
	3,6			
2,7				

1(d) R.F. test

frequency = 2,5 MHz

Temperature = 23°C

Region	Breakdown (peak KV)	Average breakdown	Thickness mm
over- hang	2,9	2,85KV (peak) ≈ 31,3KV/cm	av = 0,91mm
	2,9		
	2,3		
	3,1		
	2,9		
	3,0		
core	3,0	2,57KV (peak) ≈ 41,7KV/cm	av = 0,574mm
	2,5		
	2,2		
	3,4		
	2,3		
	2,9		
	3,0		
	2,7		
	3,0		
	2,8		
	2,9		
2,8			

Coil 2

Diamond coil for 6,6 KV motor

Insulation: Alkonex enamel plus double glass and
alkyd enamel

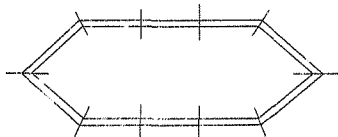
Inductance \approx 119 microHenry

Copper cross section 2,0mm x 7,3mm

9 turns

Oscillatory impulse test failure at 31 KV

Coil cut in 10 pieces \approx 4 overhang and 6 core



- 2(a) Standard Impulse Test
 IEC Standard Impulse 1,2/50 microseconds
 Temperature = $24^{\circ}\text{C} \pm 2^{\circ}\text{C}$

overhang region							
Break-down KV	Average break-down	Normalised break-down	Vari-ation	(var) ²	Thick-ness	Average thick-ness	Dielectric strength
25		1,26	0,26	0,0676			
25		1,26	0,26	0,0676			
21		1,06	0,06	0,0036			
23	19,7kV	1,16	0,16	0,0256		0,37mm	505KV/cm
14		0,71	0,29	0,0841			
12		0,60	0,40	0,1600			
18		0,91	0,09	0,0081			
core region							
28,0		1,25	0,25	0,0625			
18,9		0,84	0,16	0,0256			
17,1		0,76	0,24	0,0576			
22,8		1,02	0,02	0,0004			
30,0		1,34	0,34	0,1154			
20,3		0,91	0,09	0,0081			
25,5		1,14	0,14	0,0196			
15,7	23,5kV	0,70	0,30	0,0900		0,305mm	643KV/cm
28,0		1,13	0,13	0,0169			
30,0		1,21	0,21	0,0441			
14,0		0,56	0,44	0,1936			
27,5		1,11	0,11	0,0121			
27,0		1,09	0,09	0,0081			
26,0		1,05	0,05	0,0025			
27,0		1,09	0,09	0,0081			
18,0		0,70	0,30	0,0900			

2(b) Damped Oscillatory Test

$$f = 180 \text{ kHz} \quad T_{\frac{1}{2}} = 40 \text{ microseconds}$$

$$T_{\text{temperature}} = 24^{\circ}\text{C}$$

overhang region							
Break-down KV	Average break-down	Normalised break-down	Variation	(var) ²	Thickness	Average thickness	Dielectric strength
17,5	10,1KV	1,08	0,08	0,0064	0,42	0,390mm	413KV/cm
11,0		0,68	0,33	0,1024	0,36		
19,0		1,17	0,17	0,0289	0,39		
16,0		0,99	0,01	0,0001	0,42		
17,5		1,08	0,08	0,0064	0,39		
17,5		1,08	0,08	0,0064	0,39		
15,0		0,93	0,07	0,0049	0,39		
15,5		0,96	0,04	0,0016	0,36		
core region							
19,0	21,5KV	0,88	0,12	0,0144	0,38	0,360mm	588KV/cm
23,0		1,06	0,06	0,0036	0,34		
25,5		1,18	0,18	0,0324	0,39		
19,5		0,90	0,10	0,0100	0,38		
19,0		0,88	0,12	0,0144	0,35		
21,0		0,97	0,03	0,0009	0,37		
20,5		0,95	0,05	0,0025	0,39		
22,0		1,02	0,02	0,0004	0,36		
25,0		1,16	0,16	0,0256	0,34		
16,0		0,74	0,26	0,0676	0,37		
20,5		0,95	0,05	0,0025	0,36		
23,0		1,06	0,06	0,0036	0,36		
17,5		0,81	0,14	0,0361	0,35		
24,0		1,11	0,11	0,0121	0,35		
23,3		1,09	0,09	0,0081	0,39		
25,5	1,18	0,18	0,0324	0,37			

2(c) Radio Frequency Test

F = 1,0 MHz

Temperature = 25°C

overhang region				
Breakdown KV (peak)	Average breakdown	Thickness mm	Average thickness	Dielectric strength
3,6	2,29 KV (peak)	0,34	0,390mm	58,6KV(pk)/cm
3,4		0,40		
2,0		0,37		
2,0		0,37		
1,2		0,42		
2,0		0,40		
2,3		0,42		
1,8		0,37		
core region				
3,4	3,00 KV (peak)		0,390mm	70,9KV(pk)/cm
2,0				
3,5				
2,5				
3,0				
2,6				
3,4				
3,0				

2(d) Radio Frequency Test

F = 2,5 MHz

Temperature = 24°C

overhang region				
breakdown KV (peak)	Average breakdown	Thickness	Average thickness	Dielectric strength
2,2	2,85 KV (peak)		0,38mm	75,0KV(pk)/cm
2,6				
2,9				
2,7				
4,0				
3,2				
2,7				
2,5				
core region				
2,5	2,50 KV (peak)		0,341mm	75,1KV(pk)/cm
2,0				
1,9				
2,1				
2,9				
2,9				
3,0				
3,2				

3. Tests on Nomex M - mica-loaded polyamide fibre paper

3(a) Radio Frequency Test

Temperature = 25°C

Frequency	Breakdown	Thickness	Dielectric strength
2,0MHz	1250 V	0,130mm	92,4kV(pk)/cm
	1300 V	0,140mm	
1,0MHz	1700 V	0,139mm	122,3kV(pk)/cm
	1700 V	0,140mm	
0,5MHz	1900 V	0,139mm	139,8kV(pk)/cm
	2000 V	0,140mm	

4. Tests on Kapton Film - Polyimide (Du Pont)

4(a) Standard Impulse Test

Temperature = 25°C

Break-down KV	Average break-down	Normalised break-down	Variation	(var) ²	Thickness mm	Average thickness	Dielectric strength
7,2		0,08	0,02	0,0004	0,030		
7,5	7,4KV	1,01	0,01	0,0001	0,030	0,030mm	2,47MV/cm
7,5		1,01	0,01	0,0001	0,030		

4(b) Oscillatory Impulse Test

Temperature = 25°C

Break-down KV	Average break-down	Normalised break-down	Variation	(var) ²	Thickness mm	Average Thickness	Dielectric strength
0,0		1,04	0,04	0,0016	0,028		
7,1	0,9KV	1,01	0,03	0,0009	0,031	0,030mm	2,30MV/cm
7,0		1,01	0,01	0,0001	0,031		

4(c) Radio Frequency Tests

Temperature = 25°C

Frequency MHz	Breakdown volts (peak)	Average breakdown volts (peak)	Thickness mm	Dielectric strength KV(pk)/cm
2,0	475 450 450 440	454	0,030	168
4,0	410 400 420	410	0,028	164
1,2	490 490 510 500	497	0,030	177
0,70	550 550 570 550	555	0,030	185
1,01	560 560 570	563	0,032	176
0,91	580 580 580	580	0,032	181
0,71	590 580 610	593	0,031	192
0,52	660 640 630	643	0,030	214
0,33	630 630 630 620	628	0,028	224

Frequency MH _z	Breakdown volts (peak)	Average breakdown volts (peak)	Thickness mm	Dielectric strength KV(pk) _{cm}
5,00	540 520 520 510 510	522	0,030	174
10,0	460 400 420 440 420 450 450	434	0,029	149
7,5	480 470 470 460	470	0,030	157
1,8	480 500	487	0,029	168
power frequency 50 H _z	6800 6400 6800 5900 7600	6700	0,031	2160

5. Statistical analysis of coil sample breakdowns.

5.1 Determination of standard deviation, histogram and probability distribution of samples.

83 samples available from impulse tests (of both types) on the coil samples.

Using the formula for standard deviation

$$s = \sqrt{\frac{\sum (v - \bar{v})^2}{n-1}}$$

yielded $s = 0,1831$

Using the pre-programmed statistical function of a Hewlett Packard HP25C calculator yielded

$s = 0,1833$

It was thus assumed that

$s = 0,1832$

A histogram with an interval of 0,05 was drawn using values of breakdown normalised according to sample, test and region (core or overhang).

Breakdown intervals (normalised)	Number of readings in interval	Sample probability in interval
0,50-0,54	0	0,000
0,55-0,59	1	0,012
0,60-0,64	2	0,024
0,65-0,69	1	0,012
0,70-0,74	5	0,060
0,75-0,79	2	0,024
0,80-0,84	5	0,060
0,85-0,89	6	0,072
0,90-0,94	10	0,120
0,95-0,99	10	0,120
1,00-1,04	5	0,060
1,05-1,09	12	0,145
1,10-1,14	9	0,108

Breakdown intervals (normalised)	Number of readings in interval	Sample probability in interval
1,15-1,19	5	0,060
1,20-1,24	2	0,024
1,25-1,29	4	0,048
1,30-1,34	1	0,012
1,35-1,39	2	0,024
1,40-1,44	1	0,012
1,45-1,49	0	0,000

A normal probability distribution curve can be drawn using the values obtained from tables of erf y , the error function

$$\text{erf } y_1 = \frac{2}{\sqrt{\pi}} \int_0^{y_1} e^{-y^2} dy$$

where $y = \frac{V-V}{s\sqrt{2}}$

with V the normalised breakdown voltage and s the standard deviation i.e. 0,1832.

As the above expression applies to both sides of the probability curve, $\frac{1}{2}$ erf y must be used.

V	y	$\frac{1}{2}$ erf y	Prob($V_n - V_{n-1}$)
0,975	0,096	0,054	0,106
1,025	0,096	0,054	0,105
1,075	0,289	0,159	0,093
1,125	0,482	0,252	0,078
1,175	0,675	0,330	0,060
1,225	0,868	0,390	0,043
1,275	1,061	0,433	0,0289
1,325	1,254	0,4619	0,0178
1,375	1,447	0,4797	0,0101
1,425	1,640	0,4898	0,0054
1,475	1,833	0,4952	0,0027
1,525	2,026	0,4979	0,0012
1,575	2,219	0,4991	

5.2 Statistical estimation of coil breakdown

If a normal distribution is assumed for the breakdown of the samples then the breakdown of a coil made up of a number of such samples can be estimated.

$$\text{i.e. Prob(coil)} = \text{Prob(sample)} \times \text{no. of samples}$$

The number of samples must be estimated to be those that can be fitted into the weakest portion of the coil (usually the overhang region). Since about 20% of each sample is not active, being used for end insulation and connection, the actual number of samples must be corrected by a factor of 1,25x.

Thus for coil no. 2 the actual number of overhang samples is 32. This gives a corrected number of 40.

1% probability of coil failure therefore requires a sample probability of 40x less than this.

$$\text{i.e. Prob(sample)} = 0,00025$$

This probability in relation to the error function is

$$\begin{aligned} \text{erf } y &= 1 - 2\text{Prob(sample)} \\ &= 1 - 0,0005 \\ &= 0,9995 \end{aligned}$$

since only the lower section of the probability distribution between y and $-\infty$ is of interest.

This yields

$$y = 2,461$$

The normalised voltage corresponding to this is

$$V_n = 1 - s \sqrt{2} y$$

$$\text{if } s = 0,1832$$

$$\begin{aligned} V_n &= 1 - 0,1832 \sqrt{2} \times 2,461 \\ &= 0,362 \end{aligned}$$

i.e. if average breakdown is 16,1 KV

$$V = 5,83 \text{ KV per turn.}$$

Thus the total voltage across the coil is 9x this

i.e. 52,5 KV

Actual failure was at 31 KV

For 50% failure

$$\text{Prob}(\text{sample}) = 0,0125$$

$$\text{erf } y = 0,975$$

$$y = 1,585$$

$$V_n = 0,589$$

$$V_t = 9,49 \text{ KV}$$

$$\text{Total } V = 85,4 \text{ KV}$$

For coil no. 1

No. of samples = 24

Corrected number of samples = 30

For 1% probability

$$\text{Prob}(\text{sample}) = 0,000333$$

$$\text{erf } y = 0,999333$$

$$y = 2,47$$

$$V_n = 0,360$$

$$V_t = 8,32 \text{ KV}$$

$$\text{Total } V = 58,2 \text{ KV}$$

Actual failure was at 35 KV

For 50% failure

$$\text{Prob}(\text{sample}) = 0,0167$$

$$\text{erf } y = 0,9667$$

$$y = 1,55$$

$$V_n = 0,598$$

$$V_t = 13,82 \text{ KV}$$

$$\text{Total } V = 96,8 \text{ KV}$$

REFERENCES

- 1 Oliver, J.A., Woodson, H.H., and Johnson, J.S.,
'A Turn Insulation Test for Stator Coils'
AIEE Trans. on Power Apparatus and Systems,
Vol PAS-87, No. 3, March 1968. pp. 669-678.
- 2 Private letter. From Reid and Mitchell (Pty) Ltd.
- 3 Rüdénberg, R.
'Electrical Shock Waves in Power Systems', 1st English
edition = 4th German edition.
Harvard University Press, 1968.
- 4 Lewis, W.W.
'The Protection of Transmission Systems against
Lightning'. 1st ed.
Dover Publications, 1965.
- 5 Beck, E.
'Lightning Protection for Electric Systems', 1st ed.
McGraw-Hill Book Company, 1954.
- 6 Eriksson, A.J.
'Overvoltage Surges in Industrial Complexes'.
Symposium on High Voltage Engineering in South Africa,
Johannesburg, 18-19 November 1974.
- 7 Kano, I., Hakamada, T., Kurasawa, Y., and Sugawara, H.,
'Switching Surge Phenomena in Induction Motor
Windings and Their Endurance',
Hitachi Review, Vol. 24, No. 5, 1975, pp. 225-233.
- 8 British Standards Specification B.S. 923.

- 9 American Standards for Transformers, Regulators and Reactors,
American Standards Association C57.22, 1948.
- 10 I.E.C. Specification 60.
- 11 Foust, C.M. and McAuley, P.H.
'Recommendations for H.V. Testing by Subcommittee on Correlation of Laboratory Data of EEL and NEMA'.
AIEE Trans, Vol. 59, 1940, pp. 598-602.
- 12 Alston, L.L. et al.
'High Voltage Technology', Chapter 6, Section 8.
Oxford University Press, 1968.
- 13 Kuffel, E., and Abdullah, M.,
'High Voltage Engineering', 1st edition,
Pergamon Press, 1970.
- 14 Lewis, W.W., Weisman, R.W. and Rudge, W.J.
'Protection of Rotating A.C. Machines against Travelling Wave Voltages due to Lightning'
AIEE Trans, Vol. 52, 1933. pp. 434-440.
- 15 Griscom, S.B. et al.
'Five Year Field Investigation of Lightning Effects on Transmission Lines'
AIEE Trans, Power Apparatus and Systems, Vol. PAS 84,
No. 4, April 1965. pp. 257-280.
- 16 Martzloff, and Hahn,
'Surge Voltages in Residential and Industrial Power Circuits',
IEEE Trans, Power Systems and Apparatus, Vol. PAS 89,
No.6, Jul/Aug 1970, pp. 1049-1056.

- 17 Harder, E.L. and Clayton, J.M.
 'Lightning Phenomena',
 Westinghouse Engineer,
 Vol. 2, July 1951. pp. 106-111.
- 18 Melan, D.J.
 'Physics of Lightning' 1st ed., Chapter 11,
 English Universities Press, 1963.
- 19 McEachron, K.B.,
 'Lightning to Empire State Building',
 AIEE Trans. Vol. 60, 1941, pp. 885-889.
- 20 McCann, G.D.,
 'The Measurements of Lightning Currents in Direct
 Strokes',
 AIEE Trans, Vol. 63, 1944, pp. 1157-1164.
- 21 Bellaschi, P.L.,
 'Lightning Surges Transferred from One Circuit to
 Another through Transformers',
 AIEE Trans, Vol. 62, Dec. 1943, pp. 731-738.
- 22 Heller, B. and Veverka, A.,
 'Surge Phenomena in Electrical Machines', 1st ed.
 Hiff Books, 1968.
- 23 Wellauer, M.,
 'The Voltage Stresses in the Entrance Coils of Windings
 on the Occurrence of Impulse Voltages of Different
 Steepness',
 Bulletin Oerlikon No. 270, pp. 1823-1829
 (continued) No. 271, pp. 1843-1848
- 24 Friedlander, E.,
 'Travelling Waves in H.V. Alternator Windings',
 IEE Journal, Vol. 89 part 2, 1942, pp. 492-508
 and Vol. 90 1943, pp. 83-130.

- 25 Meyer, H.,
'Behaviour of Rotating Machinery Windings on the Occurrence of Travelling Waves',
Brown-Boveri Review, Vol. 30, 1943. pp. 279-286.
- 26 Poritsky, Ahotti, P.A. and Jerrard,
'Field Theory of Wave Propagation along Coils',
AIEE Trans, PAS 72, Oct. 1953. pp. 930-938.
- 27 Blume, I. and Boyajian, A.,
'Abnormal Voltages Within Transformer Windings',
AIEE Trans, Vol. 38, 1919. p 577.
- 28 Palueff, K.K.,
'The Influence of Transient Voltages on Transformer Design',
AIEE Trans, Vol. 44S, July 1929, p 681.
- 29 Hodnette, J.K.,
'Effect of Surges on Transformer Windings',
AIEE Journal, Nov. 1929, p 829.
- 30 Waldvogel, P. and Rouxel, R.,
'A New Method of Calculating the Electric Stresses in a Winding Subjected to a Surge Voltage',
Brown Boveri Review, Vol. 43, 1956. pp. 206-213.
- 31 Rylander, J.L.,
'High Frequency Voltage Test for Insulation of Rotating Electrical Apparatus',
AIEE Trans, Vol. 45, 1926. pp. 459-465.
- 32 Wellauer, M.,
'A New Arrangement for Testing the Insulation of the Turns of Machine Coils',
Bull. Verlikon, No. 251, Vol. XXIV, pp. 1624-1626.

33. Kranke, D. and Schuler, R.,
'A Method for Checking the Turn Insulation of Form-wound Coil Windings for High Voltage Machines',
Brown Boveri Review, Vol 57, April 1970, pp. 191-196.
34. Sexton, R.M. and Alke, R.J.,
'Detection of Turn to Turn Faults in Large H.V. Turbine Generators',
AIEE Trans, Vol. 70, 1951. pp. 270-274.
35. Catlin, E.H. and Rohats, N.,
'Winding Insulation Tester for D.C. Armatures',
AIEE Trans, Vol. 70, 1951, pp. 465-468.
36. Moses, G.L. and Harter, E.F.,
'Winding Fault Detection and Location by Surge Comparison Testing',
AIEE Trans, Vol. 64, July 1945, pp. 499-503.
37. Reynolds, D.J., Alke, R.J. and Buchanan, L.W.,
'Testing Insulation with the Surge Comparator',
Westinghouse Engineer, July 1951.
38. Weed, H.R.,
'Electronic Surge Testing of Universal Armatures with Mild Detection',
AIEE Trans, Vol. 78 part IIIB, Dec. 1959, pp. 1219-1226.
39. Strain, R.A.,
'Some Aspects of Surge Comparison Testing of Fractional Horsepower Motor',
AIEE Trans, Vol. 75 part III, Oct. 1956, pp. 917-921.
40. Kritzingor, J.J.,
'The Breakdown Mechanism of Long Sparks in Air',
Ph.D. Thesis University of the Witwatersrand, Johannesburg.

- 41 Jones, R.F.B. and Ahmed, M.,
'Impulse Testing of Motor Coils',
Dissertation prepared in partial fulfilment of BSc(Eng)
degree, 1970, Dept. Elec. Eng., University of the Wit-
watersrand, Johannesburg.
- 42 Thomas, H.A.,
'Theory and Design of Valve Oscillators for Radio
and other Frequencies',
Chapman and Hall, 1st edition, 1944. p 32, 37-38, 40.
- 43 Terman, F.E.,
'Electronic and Radio Engineering',
McGraw-Hill, International Student Edition, 4th Edition,
pp. 489-496.
- 44 Pimm, J.A.,
'The Electrical Breakdown Strength of Air at V.H.F.',
Proc IEE Vol. 96 (III), 1949. pp. 117-129.
- 45 Fatehchand, R.R.T.,
'The Electrical Breakdown of Gaseous Dielectrics at
High Frequencies',
Proc IEE Vol. 104 (c), 1957. pp. 489-495.
- 46 Bright, A.W. and Huang, H.C.,
'Formative Time-lag Studies with High Frequency Dis-
charges',
Proc IEE, Vol. 102 (c), 1955. pp. 42-45.
- 47 Peek, F.W.,
'Dielectric Phenomena in High Voltage Engineering',
McGraw-Hill, 2nd edition, 1920. p 177.

Author Hopkins MJ

Name of thesis Testing of the Inter-Turn Insulation of High Voltage Induction Motor Coils

PUBLISHER:

University of the Witwatersrand, Johannesburg

©2013

LEGAL NOTICES:

Copyright Notice: All materials on the University of the Witwatersrand, Johannesburg Library website are protected by South African copyright law and may not be distributed, transmitted, displayed, or otherwise published in any format, without the prior written permission of the copyright owner.

Disclaimer and Terms of Use: Provided that you maintain all copyright and other notices contained therein, you may download material (one machine readable copy and one print copy per page) for your personal and/or educational non-commercial use only.

The University of the Witwatersrand, Johannesburg, is not responsible for any errors or omissions and excludes any and all liability for any errors in or omissions from the information on the Library website.